Journal of proteome research

Article

Cite This: J. Proteome Res. 2019, 18, 3142−3155

pubs.acs.org/jpr

# Changes in the Turnover of the Cellular Proteome during Metabolic Reprogramming: A Role for mtROS in Proteostasis

Ana García-Aguilar,[†] Inmaculada Martínez-Reyes,[†] and José M. Cuezva*

Departamento de Biología Molecular, Centro de Biología Molecular Severo Ochoa (CSIC-UAM), Centro de Investigación Biomédica en Red de Enfermedades Raras CIBERER-ISCIII, Instituto de Investigación Hospital 12 de Octubre (i+12), Universidad Autónoma de Madrid, 28049 Madrid, Spain

Supporting Information

**ABSTRACT:** The role played by protein turnover in metabolic reprogramming is unknown. Herein, using a SILAC approach, we have studied the changes in the half-life of 266 proteins of energy metabolism and of translation during the metabolic switch induced by the prolyl hydroxylases inhibitor dimethyloxalyl-glycine (DMOG). DMOG induces HIF-1$\alpha$ expression and triggers the activation of glycolysis and the concurrent inhibition of mitochondrial respiration in colon cancer cells. Changes in the activity of energy provision pathways correlated with increased turnover rates of glycolytic enzymes and the stabilization of mitochondrial proteins. Moreover, reprogramming also stabilized the proteins of translation. The partial DMOG-mediated arrest of the synthesis of mitochondrial and translation proteins results from the inhibition of the mTORC1/p70SK/S6 signaling pathway. In contrast, DMOG stimulated the synthesis of glycolytic enzymes, emphasizing the opposite and differential regulation of the two pathways of energy provision. Addition of MitoQ, a mitochondrial reactive oxygen species (mtROS) scavenger, stabilized the turnover of cellular proteins similarly as when protein degradation is inhibited with leupeptin, a serine-protease inhibitor. Overall, the results show that the higher the activity of a pathway the lower is the half-life of the proteins involved and suggest a role for mtROS in cellular proteostasis. Data are available via ProteomeXchange with identifier PXD013482.

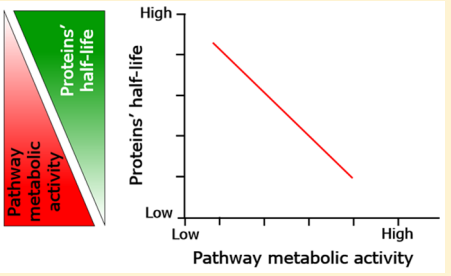


**KEYWORDS:** *ATP synthase, glycolysis, mitochondrial ROS, mTORC1, prolyl hydroxylases, SILAC*

## INTRODUCTION

Tumor cells reprogram metabolism to cope with the increased metabolic demand imposed by uncontrolled proliferation and for adaptation to the microenvironment.[1−3] Under hypoxia, cancer cells activate the hypoxia-inducible transcription factor-1$\alpha$ (HIF-1$\alpha$), a master regulator of the hypoxic response, which mediates the regulation of the expression of genes involved in angiogenesis, erythropoiesis, metabolism, cell survival and proliferation.[4−7] The activation of HIF-1$\alpha$ triggers the specific translation of selective mRNAs encoding proteins of metabolism involved in promoting a shift from oxidative phosphorylation (OXPHOS) to glycolysis to maintain energy production.[8] Under normal oxygen tension, HIF-1$\alpha$ is hydroxylated by a group of enzymes called prolyl-4-hydroxylases (PHD).[9] Hydroxylation of HIF-1$\alpha$ allows its recognition by a protein-ubiquitin ligase complex containing the tumor suppressor von Hippel-Lindau E3, promoting its ubiquitination and proteasomal degradation.[10,11] In contrast, under hypoxic conditions, the activity of PHDs is inhibited resulting in HIF-1$\alpha$ stabilization.[10] Dimethyloxaloylglycine (DMOG) is a competitive inhibitor of the prolyl and asparaginyl hydroxylases that promotes HIF-1$\alpha$ stabilization and has been extensively used to study hypoxia driven effects. In fact, DMOG reprograms energy metabolism by repressing mitochondrial respiration while activating glycolysis in cardiomyocytes[12] and in cancer cell lines.[13,14]

Proteins are in dynamic equilibrium in vivo as they are continuously synthesized and degraded during the lifetime of the organism.[15] The constant recycling (turnover) of proteins is an energy consuming process that offers a safeguard strategy against protein damage and for rapid cellular adaptation to changes in the environment.[16] The mammalian target of rapamycin complex 1 (mTORC1) signaling pathway is key in coordinating anabolic and catabolic processes to maintain homeostasis including the regulation of protein synthesis and degradation.[17−19] Proper proteome dynamics is necessary for normal development and health maintenance,[20,21] being influenced by a large number of cell-type regulated processes and by the biochemical properties of the molecules itself.[22] Conversely, dysregulation of protein turnover has been implicated in aging and in the pathogenic accumulation of protein aggregates in neurological diseases.[23,24] Because proteins can turnover rapidly, even when they are in steady state, we have used metabolic labels that are incorporated or lost from the proteins to measure their turnover rates.[25] In this study, we have used DMOG as a tool to investigate the potential role of protein turnover in metabolic reprogramming. We demonstrate that the turnover rate of glycolytic enzymes is significantly accelerated during metabolic rewiring to an

**Received:** April 12, 2019
**Published:** July 11, 2019






DOI: 10.1021/acs.jproteome.9b00239
J. Proteome Res. 2019, 18, 3142−3155

enhanced glycolysis by DMOG treatment. In contrast, the turnover of the mitochondrial, ribosomal, and other translation-related proteins is significantly slowed-down concurrently with the inhibition of the mTORC1 pathway. In other words, the turnover of enzymes of energy metabolism inversely correlates with the flux of matter and energy through the metabolic pathway in which the proteins participate. Incubation of the cells with a mitochondrial ROS (mtROS) scavenger or the inhibition of serine proteases significantly decelerate the overall turnover of cellular proteins, suggesting the implication of oxidative damage of proteins as a factor involved in the regulation of protein turnover during metabolic reprogramming.

## MATERIALS AND METHODS

### Cellular Treatments

Human colorectal carcinoma HCT116 cells were grown at 37 °C and 5% $CO_2$ in McCoy's 5A media supplemented with 10% fetal bovine serum. Cells were left untreated (CRL), treated with 1 mM dimethyloxaloylglycine (DMOG) (Enzo Life Science) for 24−48 h, 20 nM MitoQ for 48 h or 200 μM leupeptin (Sigma) for 24 h. After cell recovery and lysis (see protein extraction), protein concentration was determined with the Bradford reagent.

### Determination of Glycolysis and Cellular Respiration

The initial rate of lactate accumulation in the culture media was used as an index of glycolysis.[26] Oxygen consumption rates (OCR) were determined in a XF24 Extracellular Flux Analyzer (Seahorse Bioscience). Cells were seeded in the microplates for 24h and the OCR determined after the addition of 6 μM oligomycin, 0.75 mM 2,4-dinitrophenol (DNP), 1 μM rotenone plus 1 μM antimycin.[27]

### Western Blots

Cellular extracts were fractionated by SDS/PAGE and transferred on to PVDF membranes. The primary monoclonal antibodies used in this study were: anti-Hsp60 (clone 17/9−15 G1, 1:5000), anti-β-F1-ATPase (clone 11/21−7 A8, 1:1000) and anti-GAPDH (1:20 000).[28] Other antibodies used were anti-HIF-1α (1:150) from Santa Cruz Biotechnology, anti-CDK1 (1:1000), anti-p-CDK1 (1:1000), anti-eIF3A (1:1000), anti-eIF4E (1:1000), anti-p-mTOR (1:500), anti-mTOR (1:1000), anti-p-P70S6K (1:1000), anti-P70S6K (1:1000), anti-S6 (1:1000), anti-p-S6 (1:1000), anti-p-4EBP1 (1:1000) and anti-4EBP1 (1:1000) from Cell signaling, anti-eIF3D (1:1000) from Acris, anti-ENO1 (1:1000) from Abyntek Biopharma and anti-β-actin (1:10 000) and eIF3E (1:1000) from Sigma. Anti-P0 (1:1000) and anti-P1/P2 (1:1000) antibodies were kindly provided by Dr. J.P.G. Ballesta (CBMSO). Peroxidase-conjugated antimouse or antirabbit IgGs (Nordic Immunology; 1:3000) were used as secondary antibodies. The blots were revealed using a chemiluminescence detection method (ECL, Invitrogen). Quantification of the immunoreactive bands (arbitrary units) was accomplished using a Kodak DC120 Zoom digital camera and the Kodak 1D Image Analysis Software for Windows.

### Determination of Cell Proliferation

The incorporation of 5-ethynyl-20deoxy-uridine (EdU) into cellular DNA was determined using the Click-iT EdU Flow Cytometry Assay Kit (Molecular Probes). Cells were analyzed in a FACScan. For each analysis 10 000 events were recorded.

### Determination of the Rates of β-F1-ATPase and GAPDH Synthesis and Turnover Using $^{35}$S-Met

Cells were incubated 20 min in cysteine-methionine-free medium. Metabolic labeling was performed by adding an aliquot of medium supplemented with 0.65 mCi of $^{35}$S-Met/mL. For the determination of the rates of protein synthesis incorporation of the tracer was allowed during 20 min in the absence or presence of DMOG.[28] For pulse-chase experiments, incorporation of the label was for 1 h, and after washing the radioactive medium cells were recovered at the indicated time points and resuspended in RIPA buffer (0.5 M NaCl, 2% Triton X-100, 0.1 M Tris-HCl pH 8.0, 0.2% SDS, 1% Na-DOC) supplemented with protease inhibitor cocktail (Roche) and freeze−thawed three times. The radioactivity incorporated into TCA precipitable protein was also determined. Immunoprecipitations were carried out from 100 μg protein of cellular extracts using G-sepharose precoated with 6 μg of the IgGs of the corresponding monoclonal antibodies.

### Stable Isotope Labeling with Amino Acids in Cell Culture (SILAC)

HCT116 cells were grown in McCoy's 5A SILAC media containing L-glutamine deficient in both L-arginine and L-lysine (Thermo Fisher) and supplemented with 10% dialyzed fetal bovine serum (dFBS) (Thermo Fisher). L-arginine and L-lysine were added in either light (Arg0, Sigma, A5006; Lys0, Sigma, L5501) or heavy form (Arg10, Thermo Fisher, 89990; Lys8, Thermo Fisher, 88209). Trypsin-EDTA was avoided at all stages of passaging. Proteins were tested for higher than 98% incorporation of the heavy labeled amino acids after nine passages by mass spectrometry.

To assess the effect of DMOG on protein turnover, three p60 plates of treated or untreated cells were mixed at the following time points: 0, 6, 12, 24, and 48 h and further processed for protein extraction and identification. To assess the effect of MitoQ, MitoQ+DMOG and leupeptin on protein turnover, cells treated as indicated were sampled at 0, 6, 12, and 24 h.

### Protein Extraction and Digestion for SILAC

For protein extraction 20 × $10^6$ cells/mL was lysed with 50 mM Tris-HCl pH 8.0 containing 150 mM NaCl, 0.02% sodium azide, 0.1% SDS, 1% NP-40, 0.5% sodium deoxycholate, the complete protease inhibitor cocktail EDTA-free (Roche) and the Phosphatase Inhibitor Cocktail (Sigma-Aldrich) for 15 min on ice. Extracts were centrifuged at 11 000*g* for 15 min at 4 °C. Protein extracts (30 μg), were suspended in 100 μL of sample buffer, and then applied onto 1.2 cm wide wells of a conventional SDS-PAGE gel (0.75 mm-thick, 4% stacking, and 10% resolving). The run was stopped as soon as the front entered 3 mm into the resolving gel to concentrate the proteome. The band was visualized by Coomassie staining (GelCode Blue Stain Reagent_Thermo-Fisher), excised, cut into cubes (2 × 2 mm), and placed in 0.5 mL microcentrifuge tubes.[29] The gel pieces were destained in acetonitrile:water (1:1), were reduced with 10 mM DTT for 1 h at 56 °C and the thiol groups were alkylated with 50 mM iodoacetamide for 1 h at room temperature in the dark, followed by in situ digestion with sequencing grade trypsin (Promega, Madison, WI).[30] Gel pieces were shrunk using acetonitrile and dried out in a speedvac. The dried gel pieces were reswollen in 50 mM ammonium bicarbonate pH 8.8 with 60 ng/μL trypsin at 5:1 protein:trypsin (w/w) ratio. The tubes were kept in ice for 2 h and incubated at 37 °C for 12 h.



DOI: 10.1021/acs.jproteome.9b00239
J. Proteome Res. 2019, 18, 3142−3155

Digestion was stopped by the addition of 1% trifluoroacetic acid. Supernatants were dried-down and then desalted onto OMIX Pipette tips C18 (Agilent Technologies) until the mass spectrometric analysis.

### Reverse Phase-Liquid Chromatography RP-LC−MS/MS Analysis (Dynamic Exclusion Mode)

The desalted protein digest was dried, resuspended in 10 μL of 0.1% formic acid and analyzed by RP-LC−MS/MS (reverse phase liquid chromatography tandem-mass spectrometry) in an Easy-nLC II system coupled to an ion trap LTQ-Orbitrap-Velos-Pro hybrid mass spectrometer (Thermo Scientific). The peptides were concentrated (online) by reverse phase chromatography using a 0.1 mm × 20 mm C18 RP precolumn (Thermo Scientific), and then separated using a 0.075 mm × 250 mm C18 RP column (Thermo Scientific) operating at 0.3 μL/min. Peptides were eluted using a 220 min dual gradient: from 5 to 25% solvent B in 135 min and from 25 to 40% solvent B in 45 min. The gradient was followed by 40 to 100% solvent B in 2 min, 18 min in 100% solvent B, from 100 to 5% solvent B in 2 and 18 min in 5% solvent B (Solvent A: 0,1% formic acid in water, solvent B: 0,1% formic acid, 80% acetonitrile in water). ESI ionization was done using a Nanobore emitter Stainless Steel ID 30 μm (Proxeon) interface.[31] The Orbitrap resolution was set at 30.000. Peptides were detected in survey scans from 400 to 1600 amu (1 μscan), charge state rejection +1, collision-induced dissociation (CID) fragmentation mode in linear ion trap (LIT) followed by 20 data dependent MS/MS scans (Top 20), using an isolation width of 2 u (in mass-to-charge ratio units), normalized collision energy of 35%, and dynamic exclusion applied during 60 s periods.

### Protein Identification

Protein identification from raw data was carried out using PEAKS Studio 8.5 software (Bioinformatics Solutions Inc.).[32−34] Database search was performed against uniprot-*Homo sapiens*.fasta 12/03/2018 containing 71790 sequences (decoy-fusion database). The following constraints were used for the searches: tryptic cleavage after Arg and Lys, up to two missed cleavage sites, and tolerances of 20 ppm for precursor ions and 0.6 Da for MS/MS fragment ions with a filter charge between 2 and 4 and the searches were performed allowing optional Met oxidation, Cys carbamidomethylation and $^{13}C(6)$ $^{15}N(2)$ K, $^{13}C(6)$ $^{15}N(4)$ R Silac Label. False discovery rates (FDR) for peptide spectrum matches (PSM) was limited to 0.01. Only those proteins with at least two distinct peptides being discovered from LC/MS/MS analyses were considered reliably identified.

### Quantification of Protein Turnover

Quantitation of SILAC labeled peptides was performed with PEAKS Studio 8.5 search engine (Bioinformatics Solutions Inc.),[32−34] selected "Precursor Ion Quantification SILAC" under the "Quantifications" options. We use NO normalization mode. Charge between 2 and 4. The −10LogP, Quality, and Average Area were used for Feature vector filter and Significance (Peaks Q method) for Protein filter. For the protein quantification we consider protein groups for peptide uniqueness, use only unique peptides. The H/L ratio for each protein was determined by PEAKS Studio 8.5 as the median of all of the peptides assigned to the protein.[35,36] We used the time-dependent decay of labeled peptides (ratio H/H+L) to measure the $t_{1/2}$ for each protein following the detailed protocol in the literature.[37] In cells treated or not with DMOG the time points sampled after addition of light medium were 0, 6, 12, 24, and 48 h (experiment 1, see Supplemental Tables S1−S3). In cells treated with leupeptin or MitoQ (experiment 2, see Supplemental Tables S4−S7) or MitoQ plus DMOG (experiment 3, see Supplemental Tables S4−S7) the time points sampled after the addition of the light medium were 0, 6, 12, and 24 h.

### Bioinformatics Analysis

We used the GeneCodis web tool[38−40] to analyze the pathways more affected by DMOG treatment.

### Preparation and LC-ESI-MS/MS Identification of Ribosomal Proteins

Cells at 80% confluence were harvested and incubated in a buffer containing 250 mM sucrose, 250 mM KCl, 5 mM $MgCl_2$, 50 mM Tris·Cl, pH 7.4 and NP-40 0.7% (v/v). The nuclear fraction was removed and the cytoplasmic fraction was centrifuged at 12,500*g* to remove the mitochondrial fraction. The concentration of the postmitochondrial fraction was then adjusted to 0.5 M KCl to disrupt most interactions between ribosomes and other proteins of other cell compartments. Finally, ribosomes were purified through a 0.5 M KCl sucrose cushion by ultracentrifugation. The purification of the ribosomal fraction was validated by one-dimensional SDS polyacrylamide gel electrophoresis (SDS-PAGE). Protein extracts were precipitated in methanol-chloroform and dissolved in 8 M urea, 25 mM ammonium bicarbonate, reduced and alkylated with iodoacetamide, according to a method previously described.[41] Urea concentration was reduced to 2 M with 25 mM ammonium bicarbonate (final volume 40 μL) and the samples digested overnight at 37 °C with recombinant MS-grade trypsin (Sigma-Aldrich), with a ratio of 25:1. After digestion, samples were desalted using ZipTip (Merck) as described. Nano LC-ESI-MS/MS analysis of the trypsin digested ribosomal fraction was performed using an Eksigent 1D-nanoHPLC coupled to a 5600TripleTOF QTOF mass spectrometer (ABSciex, Framinghan, MA, USA). The analytical column used was a silica-based reversed phase column Eksigent chromXP 75 μm × 15 cm, 3 μm particle size and 120 Å pore size. The trap column was a chromXP, 3 μm particle diameter, 120 Å pore size, switched online with the analytical column. The loading pump delivered a solution of 0.1% trifluoroacetic acid in 98% water/2% acetonitrile (LabScan, Gliwice, Poland) at 30 μL/min. The nanopump operated under gradient elution conditions at a flow-rate of 300 nL/min, using 0.1% formic acid (Fluka, Buchs, Switzerland) in water as mobile phase A, and 0.1% formic acid in 80% acetonitrile/20% water as mobile phase B. Gradient elution was isocratic conditions of 96% A: 4% B for 5 min, a linear increase to 40% B in 60 min, followed by a washing step of 7 min of 95% B. Injection volume was 5 μL. The LC system was coupled via a nanospray source to the mass spectrometer. Full scan ($m/z$ 350−1250) MS spectra followed by tandem MS CID spectra of the 25 most abundant ions were obtained in data-dependent acquisition mode. MS and MS/MS data were used to search against the UniprotKb database using a Mascot v.2.3.02 (Matrix Science, London, UK) containing the sequences of interest. Peptides with scores above threshold were selected, and based on these individual scores protein identifications were assigned. Search parameters were carbamidomethyl cysteine as fixed modification and oxidized proline and methionine as variable ones. Peptide mass



DOI: 10.1021/acs.jproteome.9b00239
J. Proteome Res. 2019, 18, 3142−3155

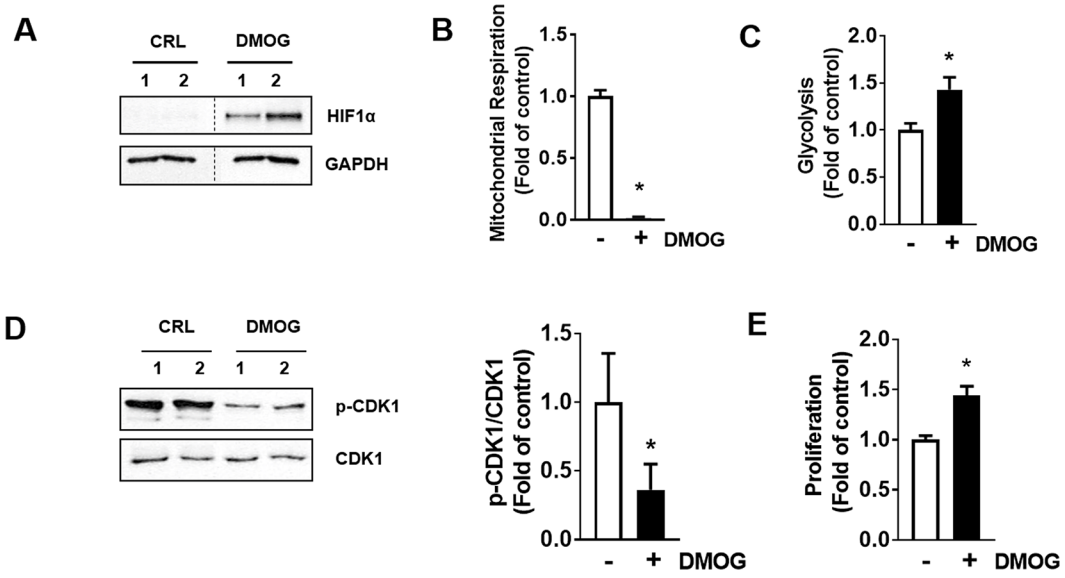


**Figure 1.** DMOG promotes a glycolytic switch and induces cellular proliferation.HCT116 cells were treated with 1 mM DMOG for 24 h or left untreated. (A) Western blot analysis of HIF-1$\alpha$ expression in two different preparations. GAPDH is shown as loading control. (B,C) Oxygen consumption (B) and lactate production (C) rates. The results shown are means ± SEM ($n$ = 6−10). (D) Western blot analysis of p-CDK1 and CDK1. The histogram shows the p-CDK1/CDK1 ratio normalized to the mean value in untreated cells. The results are means ± SEM ($n$ = 4). (E) Cellular proliferation determined by the incorporation of EdU into DNA. *$p$ < 0.05 when compared to nontreated by Student's $t$ test.

tolerance was set at 25 ppm and 0.6 Da for MS and MS/MS spectra, respectively, and 1 missed cleavage was allowed.

### RNA Extraction and Quantification of mRNA Expression

RNA was purified from untreated and 1 mM DMOG-treated HCT116 cells with Trizol Reagent (Thermo Fisher Scientific) according to the manufacturer's instructions. Purified RNA was quantified with a Nanodrop Spectrophotometer (Thermo Fisher Scientific), and 1 $\mu$g was retrotranscribed into cDNA with the High-Capacity cDNA Reverse Transcription Kit (Thermo Fisher Scientific). mRNA levels were analyzed by real-time PCR using retrotranscribed cDNA, Fast SYBR Master Mix (Thermo Fisher Scientific) and ABI Prism7900HT sequence detection system (Thermo Fisher Scientific) at the Genomics and Massive Sequencing Facility (CBMSO-UAM). Primers used to amplify the human genes were acquired from Millipore-Sigma (KiCqStart SYBR Green Primers) for *ALDOA* (Gene ID 226, primer pair 1), *ENO1* (Gene ID 2023, primer pair 1), *GPI* (Gene ID 2821, primer pair 1), *ATP5F1* (Gene ID 515, primer pair 1), *MDH2* (Gene ID 4191, primer pair 1), *OAT* (Gene ID 4942, primer pair 1), *RPL3* (Gene ID 6122, primer pair 1), *RPL8* (Gene ID 6122, primer pair 1), *RPL15* (Gene ID 6138, primer pair 1), *RPS3* (Gene ID 6188, primer pair 1), *RPS11* (Gene ID 6205, primer pair 1), *EIF4E* (Gene ID 1977, primer pair 1), *EIF3E* (Gene ID 3646, primer pair 1), *EIF3A* (Gene ID 8661, primer pair 1), *EIF3B* (Gene ID 8662, primer pair 1) and *EIF3D* (Gene ID 8664, primer pair 1). Other primers used were: $\beta$-F1-ATPase (F 5′-CTTCA-ATGGGTCCCACCATA-3′ and R 5′-CAGCAGATTT-TGGCAGGTG-3′), $\alpha$-F1-ATPase (F 5′-GATAGAGCCG-CCTAGAACCA-3′ and R 5′-TACTCCGCAGGCGGT-ACTT-3′), LDHA (F 5′-TCTCTGTAGCAGATTTGGCAGA-3′ and R 5′-AAGAC-ATCATCCTTTATTCCGTAAA-3′), GAPDH (F 5′-AGCCACATCGCTCAGACAC-3′ and R 5′-GCCCA-ATACGACCAAATCC-3′), and $\beta$-actin (F 5′-CCAAC-CGCGAGAAGATGA and R 5′-CCAGAGGCGTACAGG-GATAG).

### Preparation of Crude Initiation Factors

$8 \times 10^6$ cells were homogenized in 0.5 mL of 20 mM Tris-HCl, pH 7.6, containing 200 mM sucrose, 100 mM NH4Cl, 5 mM magnesium acetate, 0.1 mM EDTA, 1 mM dithiothreitol, and 1 mM phenylmethylsulfonyl fluoride. Cells were centrifuged at 27 000$g$ for 30 min, and the resulting supernatant was centrifuged at 100 000$g$ for 150 min to obtain the microsomal and postmicrosomal (S-100) fractions. Pelleted microsomes were resuspended in homogenization buffer devoid of $Mg^{2+}$, extracted with 0.5 M KCl under continuous shaking for 90 min, and centrifuged at 100 000$g$ for 180 min, to recover the supernatant containing the fraction of crude initiation factors.

### Statistical Analysis

Statistical analyses were performed using a two-tailed Student's $t$ test. The results shown are mean ± SEM. A $p$ < 0.05 was considered statistically significant.

## RESULTS

### DMOG Reprograms Energy Metabolism and Enhances Cellular Proliferation

HIF-1$\alpha$ stabilization is known to enhance aerobic glycolysis.[42] We confirmed that the inhibition of prolyl-hydroxylases by DMOG treatment significantly increased HIF-1$\alpha$ levels in the human colorectal cancer cell line HCT116 (Figure 1A). Consistent with the HIF-1$\alpha$-mediated shift of energy metabolism we observed a high reduction in mitochondrial respiration (Figure 1B) and a concomitant increase in the flux of aerobic glycolysis (Figure 1C). This metabolic phenotype was accompanied by a reduction in the p-CDK1/CDK1 ratio (Figure 1D) and an increased rate of cellular proliferation (Figure 1E), indicating that cell cycle progression is favored in DMOG-treated cells. Overall, the results suggest that DMOG promotes metabolic reprogramming to facilitate cellular proliferation and cell cycle progression highlighting the relevance of the inhibition of prolyl-hydroxylases for metabolic adaptation.[43]



DOI: 10.1021/acs.jproteome.9b00239
J. Proteome Res. 2019, 18, 3142−3155

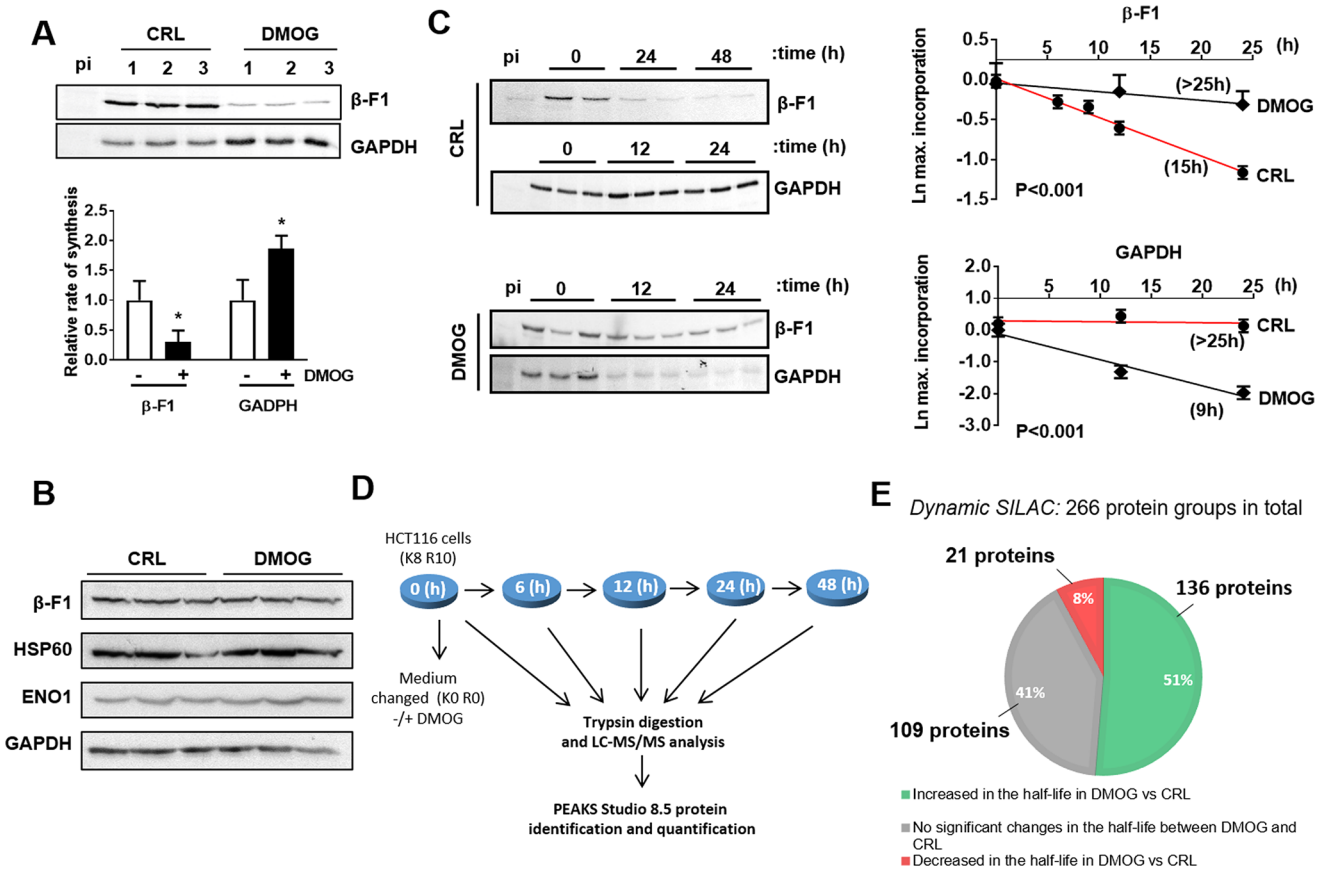


**Figure 2.** DMOG promotes opposite changes in the synthesis and turnover of proteins of energy metabolism.HCT116 cells were treated with 1 mM DMOG for 24 h or left untreated. (A) Determination of $\beta$-F1-ATPase and GAPDH synthesis rates by $^{35}$S-methionine incorporation. The fluorograms reveal the immunoprecipitated proteins in three different preparations. p.i. nonspecific immunoglobulin. The histograms show the means ± SEM ($n$ = 6). *$p$ < 0.05 when compared to nontreated cells. (B) Western blot analysis of $\beta$-F1-ATPase, HSP60, enolase 1 (ENO1), and GAPDH in three different preparations. (C) Pulse-chase experiment: After $^{35}$S-methionine labeling, $\beta$-F1-ATPase and GAPDH were immunoprecipitated at the indicated time-points for the determination of protein turnover. Two or three different preparations are shown. p.i. nonspecific immunoglobulin. The plots show the first order rate kinetics of the decay of the proteins in CRL (red lines, circles) and DMOG-treated (black lines, diamonds) cells. The $t_{1/2}$ is indicated in brackets. Results are the mean ± SEM from six determinations. $P$ < 0.001 analyzed by linear correlation of the slopes. (D) The scheme of the SILAC workflow followed to measure the turnover of cellular proteins. (E) The scheme shows the distribution of the 266 proteins studied by the effect of DMOG. Green, proteins with increased half-life; Red, proteins with decreased half-life; Gray, unaffected proteins.

## Metabolic Reprogramming Affects the Turnover of Enzymes of Energy Metabolism

Inhibition of prolyl-hydroxylases significantly reduced the initial rate of synthesis of the catalytic subunit of the mitochondrial ATP synthase ($\beta$-F1-ATPase), as assessed by the incorporation of $^{35}$S-methionine when compared to control cells (Figure 2A). In contrast, the relative rate of synthesis of the glycolytic glyceraldehyde 3-phosphate dehydrogenase (GAPDH) increased in the presence of DMOG (Figure 2A). However, and despite the high differences in the initial rates of synthesis triggered by DMOG reprogramming, we did not observe significant changes in the expression levels of $\beta$-F1-ATPase, GAPDH, the mitochondrial HSP60, and glycolytic enolase (ENO1) between control and DMOG-treated cells (Figure 2B).

Assessment of the half-life of $\beta$-F1-ATPase and GAPDH by pulse-chase experiments in the presence and absence of DMOG revealed an increase in the half-life of $\beta$-F1-ATPase in DMOG treated cells when compared to controls (Figure 2C). In contrast, DMOG promoted an increase in the turnover rate of GAPDH when compared to untreated cells (Figure 2C). Taken together, these results suggest that DMOG rewires energy metabolism by regulating the synthesis and the turnover rate of mitochondrial and glycolytic proteins while maintaining the steady state levels of the proteins involved in these processes.

## A Dynamic SILAC Approach To Assess the Turnover of the Proteome

A stable isotopic labeling amino acid (SILAC) study of the proteome was carried out to have a more complete picture of the relevance of protein turnover in metabolic reprogramming (Figure 2D). HCT116 cells were incubated in heavy medium for at least nine cell divisions, resulting in almost 100% of cells labeled with heavy arginine and lysine (R10, K8). At time 0, cells were switched to light medium (R0, K0), and incubated with or without DMOG during the indicated times (Figure 2D). For the SILAC experiments, the time-points sampled after changing the medium to the light one were at 0, 6, 12, 24, and 48 h (Figure 2D). After cellular recovery the proteins were digested with trypsin and the resulting peptides were analyzed in LC−MS/MS (Figure 2D). Switching the cells to light medium triggers the progressive replacement of heavy peptides


DOI: 10.1021/acs.jproteome.9b00239
J. Proteome Res. 2019, 18, 3142−3155

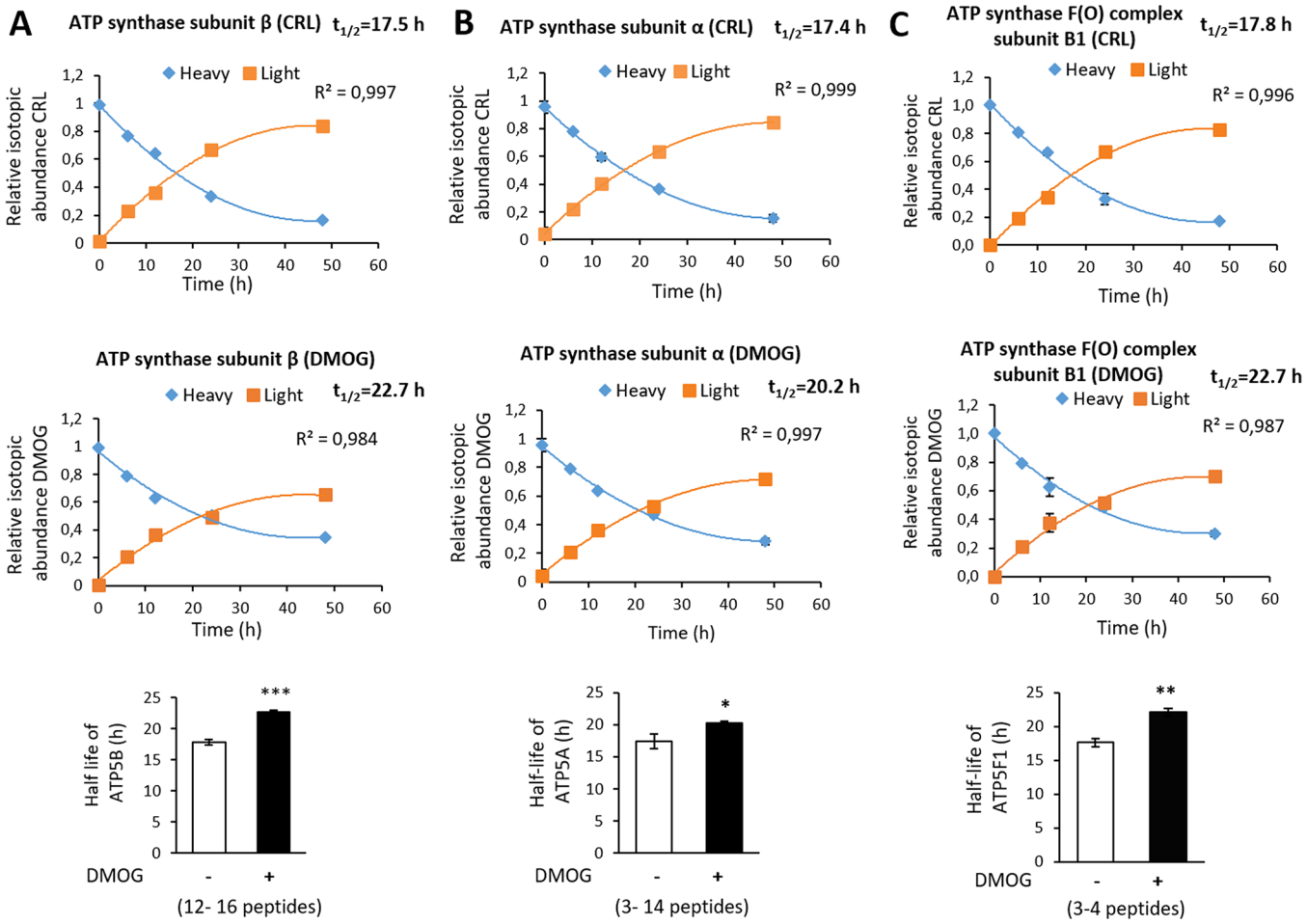


**Figure 3.** Half-life calculation for three subunits of the mitochondrial ATP synthase in response to DMOG treatment. The decay of heavy-peptides (blue diamonds) and concurrent appearance of light-peptides (orange squares) at the indicated time-points of the chase are shown for $\beta$-F1-ATPase (A), $\alpha$-F1-ATPase (B), and Fo-ATPase subunit B1 (C) for DMOG-treated and nontreated cells. The half-life ($t_{1/2}$) of each protein was calculated as the time elapsed when their peptides have the same relative isotopic abundance (RIA = 0.5). The results shown are means ± SEM of the half-lives of the different peptides studied for each subunit. *$p < 0.05$, **$p < 0.01$ and ***$p < 0.001$, when compared to nontreated by Student's $t$ test. ATP5B, ATP5A and ATP5F1, correspond to $\beta$-subunit, $\alpha$-subunit and subunit b1 of the Fo complex of the ATP synthase, respectively.

by light ones (Supplemental Figure S1). The percentage of the relative isotopic abundance (RIA) of heavy protein groups and heavy proteins identified in untreated and DMOG-treated cells over time fits a first-order kinetic (Supplemental Figure S1B). Out of the ~6000 peptide sequences monitored in the analysis, only those appearing at all time-points and conditions were selected for the study of the turnover of the proteome. The turnover of 396 and 428 proteins for DMOG-treated and untreated cells were obtained, respectively, resulting in the study of the half-life of 266 proteins in common between the two conditions (overlap of ~67%). The diagram (Figure 2E) shows that 136, 21, and 109 proteins increased, decreased or are unaffected in their half-life by DMOG treatment, respectively (Figure 2E and Supplemental Tables S1–S3).

To visualize the changes in protein turnover using the SILAC approach and the Peaks 8.5 software, we have exemplified the calculation of the half-lives of three subunits of the ATP synthase (Figure 3) and of three enzymes of glycolysis (Figure 4) following the time-dependent changes in peak-intensities of all the H and L peptides obtained for each protein (Supplemental Figure S2 and S3). The analysis indicated that DMOG induced a retardation of heavy peptides replacement for the three subunits of the mitochondrial ATP synthase $\beta$-F1, $\alpha$-F1, and b1-F(o), which means a decrease in turnover and a significant increase in their respective half-lives (Figure 3A–C). The same analysis was done for three enzymes of the glycolytic pathway (GAPDH, ALDOA and GPI) (Figure 4A–C). In this case, DMOG caused a significant increase in the decay of heavy peptides and thus an increase in the turnover of the proteins, in other words, a significant reduction in their half-lives (Figure 4A–C). Overall, these results confirmed the opposite trend in the changes induced by DMOG treatment in the turnover of $\beta$-F1-ATPase and GAPDH assessed by conventional $^{35}$S-Met labeling.

## The Inhibition of Prolyl Hydroxylases Impacts on the Turnover of Proteins Involved in Energy Metabolism

The GeneCodis web tool against Kyoto Encyclopedia of Genes and Genomes (KEGG) pathways was used to recognize the pathways that are most strongly influenced by DMOG treatment.[38−40] The analysis revealed that proteins involved in energy metabolism and in the translational machinery were the ones preferentially represented (Figure 5A). In fact, of the 38 mitochondrial proteins included in the study, ~76% of them revealed a significant increase in their half-lives as a result of DMOG treatment (Figure 5B). The rest of mitochondrial proteins detected revealed no major changes in their turnover.



DOI: 10.1021/acs.jproteome.9b00239
J. Proteome Res. 2019, 18, 3142−3155

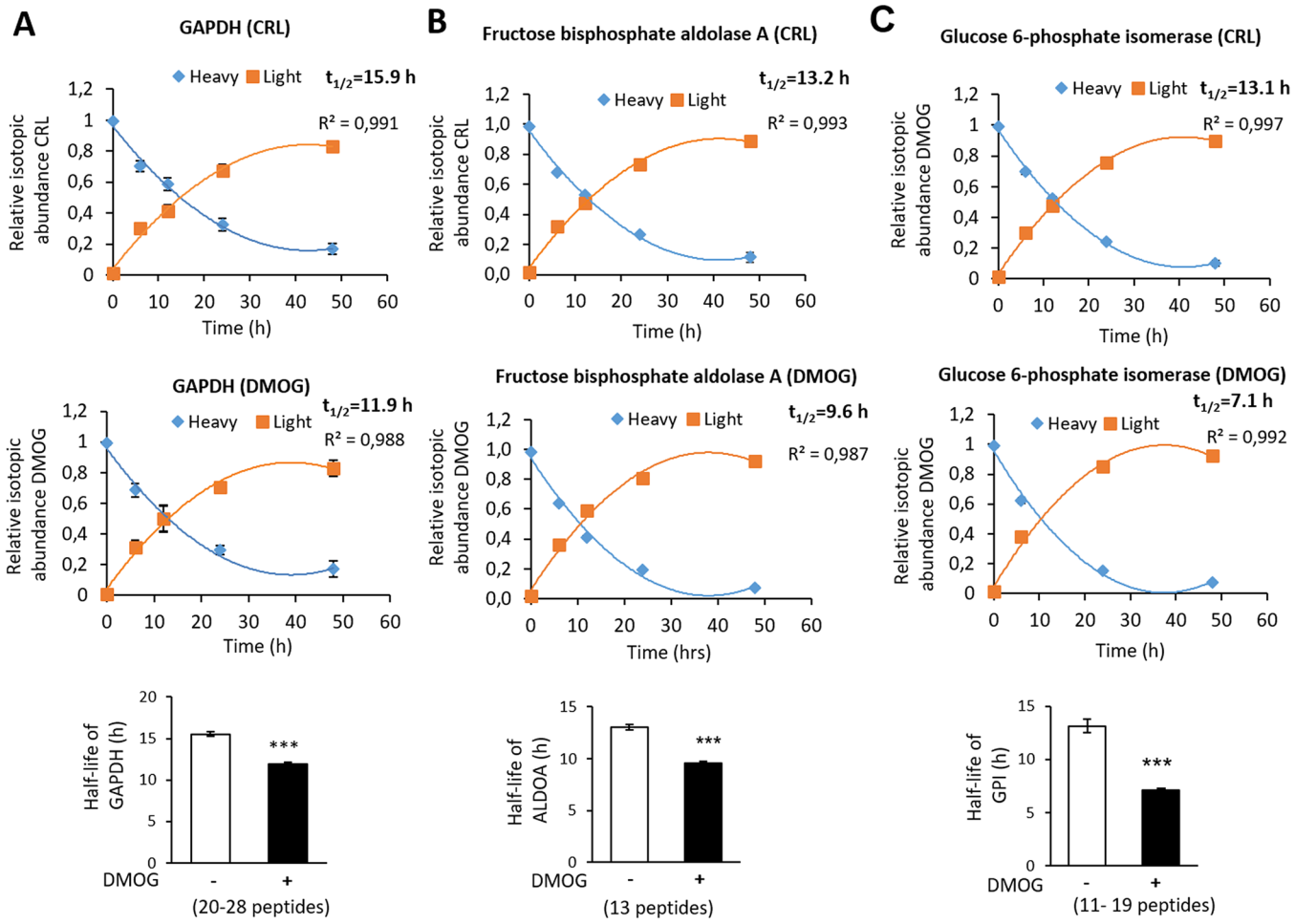


**Figure 4.** Half-life calculation for three glycolytic enzymes in response to DMOG treatment. The decay of heavy-peptides (blue diamonds) and concurrent appearance of light-peptides (orange squares) at the indicated time-points of the chase are shown for GAPDH (A), ALDOA (B), and GPI (C) for DMOG-treated and nontreated cells. The half-life ($t_{1/2}$) of each protein was calculated as the time elapsed when their peptides have the same relative isotopic abundance (RIA = 0.5). The results shown are means ± SEM of the half-lives of the different peptides studied for each protein. ***$p < 0.001$ when compared to nontreated by Student's $t$ test. GAPDH, ALDOA, and GPI correspond to glyceraldehyde-3-phosphate dehydrogenase, fructose-bisphosphate aldolase A, and glucose-6-phosphate isomerase, respectively.

Interestingly, the mitochondrial $NAD^+$-dependent malic enzyme showed a sharp reduction in its half-life (Figure 5B). In contrast to these findings, ∼67% of the glycolytic proteins studied showed a significant reduction in their half-lives upon DMOG treatment (Figure 5C). Overall, the results indicate that inhibition of prolyl hydroxylases have significant opposite effects in the regulation of the turnover of proteins involved in energy metabolism.

Determination of DMOG-induced changes in mRNA availability in some of the enzymes of energy metabolism revealed the lack of changes for the mitochondrial (Supplemental Figure S4A) and some of the glycolytic (Supplemental Figure S4B) proteins studied. Interestingly, and in the particular case of the cluster of glycolytic enzymes, we observed a significant inverse correlation between DMOG-induced changes in mRNA availability and the half-lives of the proteins (Supplemental Figure S4C).

## The Inhibition of Prolyl-Hydroxylases Promotes an Overall Stabilization of Proteins Involved in Translation

The turnover of ribosomal proteins and of translation initiation factors is of particular importance because translational control is critical for adaptation of the cells during development, differentiation, aging, and disease.[44] Of the ribosomal proteins detected, ∼94% of them showed a significant increase in their half-lives upon DMOG treatment when compared to control cells (Figure 6A). Only 2 of the 33 ribosomal proteins detected, showed significant reduction in their half-lives in DMOG-treated cells (Figure 6A). Interestingly, purified ribosomal proteins from untreated and DMOG-treated cells (Supplemental Figure.S5A) and blotting against the acidic P0, P1/P2 ribosomal proteins (Supplemental Figure S5B) indicated that their cellular abundance is not affected by DMOG treatment. This point was also confirmed by LC-ESI-MS analysis that identified 765 and 812 peptides of 92% of the ribosomal proteins in control and DMOG treated cells, respectively (Supplemental Figure S5C).

Of the initiation/elongation factors detected, 70% of them had a significant increase in their half-lives upon DMOG-treatment (Figure 6B). Interestingly, whereas proteins of energy metabolism and of the ribosome do not show relevant changes in expression after 24−48 h treatment with DMOG (Figure 2B and Supplemental Figure S5), the expression of eukaryotic translation initiation factors eIF3A, eIF3D, eIF3E, and eIF4E was significantly reduced in DMOG-treated cells (Figure 6C).



DOI: 10.1021/acs.jproteome.9b00239
J. Proteome Res. 2019, 18, 3142−3155

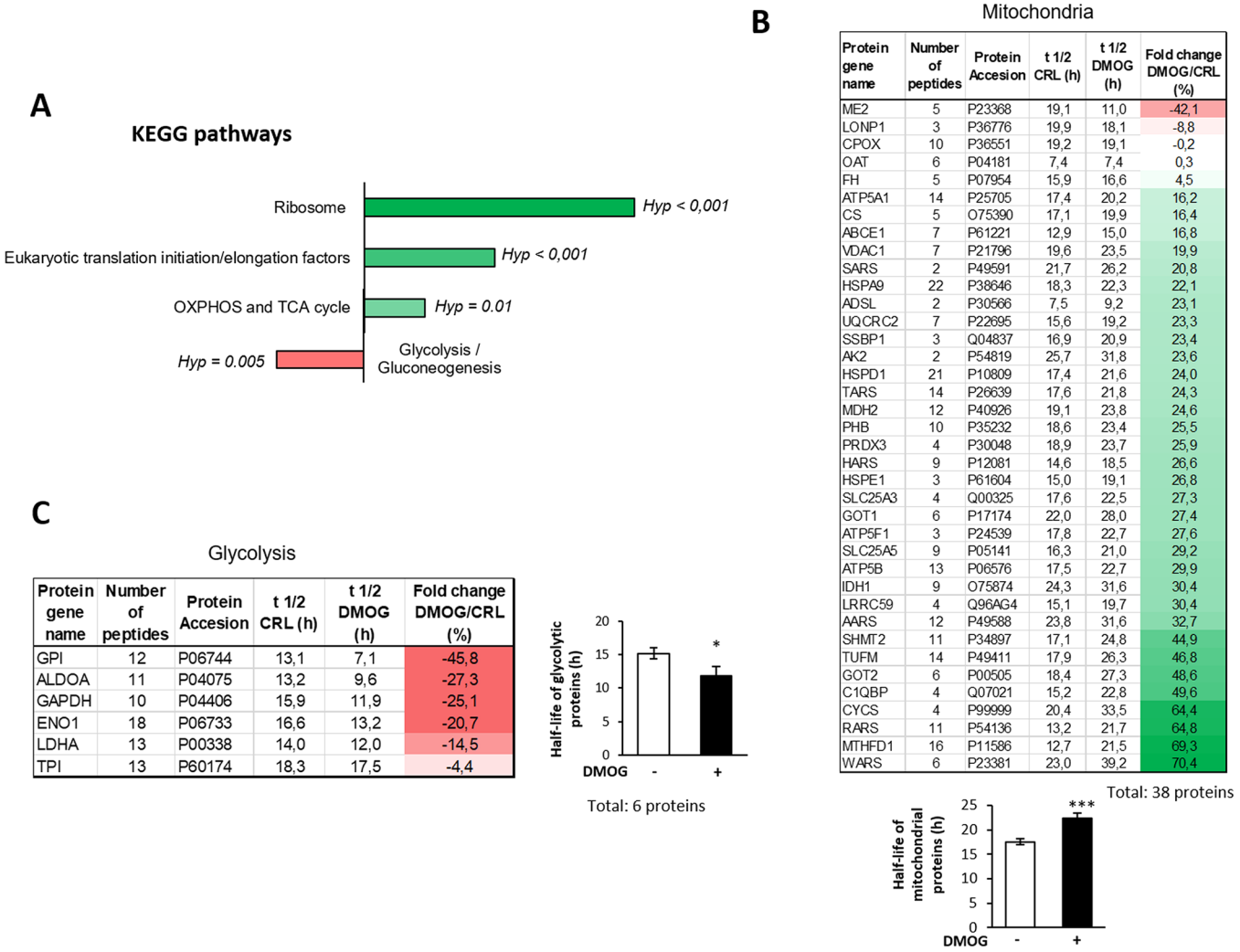


**Figure 5.** Half-life of proteins of translation and energy metabolism are major targets of DMOG treatment. (A) GeneCodis analysis against KEGG pathways. Green and red bars respectively represent the proteins with decreased and increased turnover in DMOG treated cells when compared to nontreated. Hypergeometric values (Hyp) of each KEGG pathway are also indicated. OXPHOS, oxidative phosphorylation; TCA, tricarboxylic acid cycle; KEGG, Kyoto Encyclopedia of Genes and Genomes. (B,C) The results illustrate the half-life (h) in the absence (CRL) or presence of DMOG and percentage change in the half-life of the indicated mitochondrial (B) and of glycolytic (C) protein when compared to nontreated cells as determined by the Peaks 8.5 software. The histograms show the means ± SEM of the half-lives of the total number of mitochondrial (B) and glycolytic (C) proteins included in the study. *$p$ < 0.05 and ***$p$ < 0.001, when compared to nontreated by Student's $t$ test.

Determination of DMOG-induced changes in cellular mRNA availability of proteins of the translation machinery indicated the lack of relevant differences for mRNAs encoding ribosomal proteins (Supplemental Figure 6A). In contrast, and despite the availability of mRNAs of translation initiation factors showed an increase upon DMOG treatment (Supplemental Figure 6B), their steady-state protein content was significantly decreased (Figure 6C), albeit their turnover was slowed-down (Figure 6B).

## DMOG Inhibits mTORC1 Signaling and Cap-Dependent Translation

mTORC1/S6K signaling pathway positively controls protein translation, ribosomal biogenesis and protein degradation.[45,46] The metabolic reprogramming triggered by DMOG significantly affected the phosphorylation of mTORC1 and of its downstream targets S6K, S6, and 4EBP1 (Figure 7A) suggesting the inhibition of the mTORC1 signaling pathway and its contribution in the repression of protein synthesis of mitochondrial, ribosomal and translation factors during metabolic reprogramming (Figure 7B). In contrast, the increased synthesis of glycolytic proteins in response to DMOG treatment was mTOR independent (Figure 7B).

The mitochondrial generation of ROS (mtROS) is a relevant signal to coordinate nuclear programs aimed at adapting cellular responses to changing cues[47−50] and mtROS are known to trigger the inhibition of PHD and stabilized HIF-1$\alpha$.[51−53] Analysis of the turnover of the different subcellular proteomes in the presence of MitoQ, a mitochondrial targeted ROS scavenger, indicated a significant 2-fold increase in the half-life of all the proteomes investigated, both in the absence or presence of DMOG (Supplemental Figure S7), suggesting the importance of protein oxidation in defining overall protein turnover. The effect of MitoQ however, was less relevant in the turnover of glycolytic proteins, especially under DMOG treatment (Supplemental Figure S7). In the MitoQ and MitoQ+DMOG experiments, we obtained the turnover for 192 and 371 proteins, respectively. The overlaps with the proteins found in common in the DMOG/untreated experiment were


DOI: 10.1021/acs.jproteome.9b00239
J. Proteome Res. 2019, 18, 3142−3155

A Ribosome

| Protein gene name | Number of peptides | Protein Accesion | t 1/2 CRL (h) | t 1/2 DMOG (h) | Fold change DMOG/CRL (%) |
|---|---|---|---|---|---|
| RPL23A | 5 | P62750 | 19,2 | 10,8 | -43,7 |
| RPS16 | 8 | P62249 | 17,8 | 11,9 | -33,2 |
| RPL24 | 2 | P83731 | 15,4 | 18,5 | 20,0 |
| RPL13 | 5 | P26373 | 29,9 | 35,9 | 20,4 |
| RPL7A | 8 | P62424 | 19,1 | 24,2 | 26,5 |
| RPLP0 | 7 | P05388 | 19,7 | 26,5 | 34,2 |
| RPL8 | 3 | P62917 | 17,0 | 22,9 | 35,0 |
| RPL4 | 12 | P36578 | 16,7 | 22,6 | 35,0 |
| RPL18A | 4 | Q02543 | 16,6 | 22,7 | 36,2 |
| RPS4X | 10 | P62701 | 10,9 | 15,3 | 40,5 |
| RPS18 | 8 | P62269 | 16,2 | 23,0 | 41,9 |
| RPL26 | 4 | P61254 | 17,0 | 24,3 | 43,1 |
| RPL5 | 8 | P46777 | 16,9 | 24,7 | 46,0 |
| RPL31 | 2 | P62899 | 17,3 | 25,3 | 46,1 |
| RPS19 | 3 | P39019 | 15,8 | 23,5 | 49,1 |
| RPS2 | 8 | P15880 | 15,9 | 24,3 | 53,2 |
| RPS3 | 13 | P23396 | 15,1 | 23,2 | 53,8 |
| RPL12 | 4 | P30050 | 18,2 | 28,3 | 55,5 |
| RPSA | 11 | P08865 | 15,4 | 24,0 | 55,7 |
| RPL10A | 4 | P62906 | 17,3 | 26,9 | 55,8 |
| RPS13 | 5 | P62277 | 16,3 | 25,5 | 56,4 |
| RPL21 | 2 | P46778 | 17,6 | 27,9 | 58,2 |
| RPS3A | 12 | P61247 | 14,6 | 23,3 | 59,6 |
| RPS9 | 5 | P46781 | 16,2 | 26,6 | 63,6 |
| RPS8 | 5 | P62241 | 17,4 | 28,6 | 64,7 |
| RPL3 | 5 | P39023 | 19,2 | 32,4 | 68,8 |
| RPL7 | 9 | P18124 | 18,6 | 32,0 | 71,5 |
| RPS11 | 3 | P62280 | 16,2 | 28,3 | 75,1 |
| RPL6 | 9 | Q02878 | 18,3 | 32,7 | 78,6 |
| RPS25 | 3 | P62851 | 16,3 | 29,7 | 82,4 |
| RPL14 | 3 | P50914 | 17,7 | 33,8 | 91,5 |
| RPS14 | 3 | P62263 | 16,3 | 34,9 | 113,7 |
| RPL15 | 6 | P61313 | 17,0 | 38,4 | 126,1 |

Total: 33 proteins

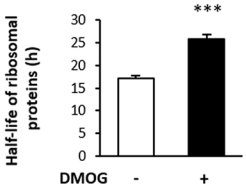


B Eukaryotic translation factors

| Protein gene name | Number of peptides | Protein Accesion | t 1/2 CRL (h) | t 1/2 DMOG (h) | Fold change DMOG/CRL (%) |
|---|---|---|---|---|---|
| EIF3H | 7 | O15372 | 12,6 | 10,9 | -13,0 |
| EIF4A1 | 17 | P60842 | 11,8 | 11,5 | -2,4 |
| ETF1 | 6 | P62495 | 14,4 | 16,0 | 11,0 |
| EIF3E | 13 | P60228 | 12,0 | 13,7 | 13,7 |
| EIF2S1 | 9 | P05198 | 16,2 | 19,4 | 19,4 |
| EIF4A3 | 15 | P38919 | 11,8 | 14,2 | 20,1 |
| EIF3A | 9 | Q14152 | 14,5 | 18,1 | 24,5 |
| EIF6 | 3 | P56537 | 12,6 | 16,3 | 29,2 |
| EEF2 | 30 | P13639 | 14,5 | 19,5 | 34,8 |
| EIF3F | 7 | O00303 | 12,9 | 17,6 | 36,7 |
| EIF3G | 4 | O75821 | 12,0 | 17,0 | 41,3 |
| EIF3L | 9 | Q9Y262 | 11,1 | 16,2 | 46,5 |
| EIF3I | 7 | Q13347 | 10,0 | 15,6 | 56,1 |
| EIF3B | 10 | P55884 | 13,0 | 20,8 | 59,8 |
| EIF2S3 | 5 | P41091 | 12,6 | 20,6 | 63,6 |
| EEF1A1 | 10 | P68104 | 17,4 | 30,1 | 72,5 |

Total: 16 proteins

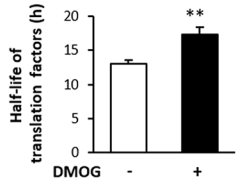


C

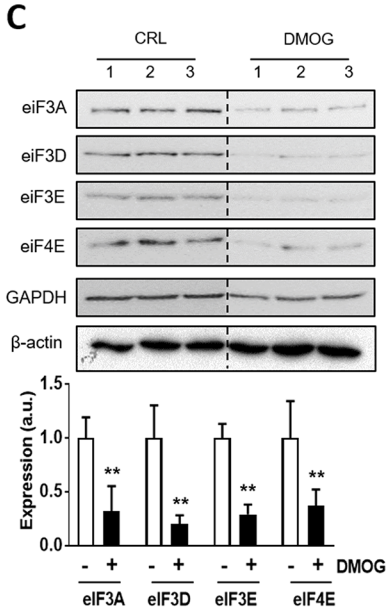


**Figure 6.** DMOG increased the half-life of ribosomal proteins and translation factors. (A,B) The results illustrate the half-life (h) in the absence (CRL) or presence of DMOG and percentage change in the half-life of the indicated ribosomal proteins (A) and translation factors (B) when compared to nontreated cells as determined by the Peaks 8.5 software. The histograms show the means ± SEM of the half-lives of the total number of ribosomal proteins (A) and translation factors (B) included in the study. $^{**}p < 0.01$ and $^{***}p < 0.001$, when compared to nontreated by Student's $t$ test. (C) Western blot analysis of the expression of the eukaryotic translation initiation factors eIF3A, eIF3D, eIF3E and eIF4E in HCT116 cells treated (+) with 1 mM DMOG for 24h or left untreated (−). GAPDH and $\beta$-actin are shown as loading controls. The histograms show the quantification of the bands (a.u.) normalized to the mean value in untreated cells. The results shown are means ± SEM ($n = 3$). $^{**}p <$ 0.01, when compared to nontreated by Student's $t$ test.

160 and 161 proteins, respectively. Supplemental Tables S4–S7 only list the glycolytic, mitochondrial, ribosomal, and translation factors in common in all the experiments.

Interestingly, the turnover of the different cellular proteomes investigated was also similarly upregulated when protein degradation was blocked with the broad spectrum protease inhibitor leupeptin that inhibits cysteine, serine and threonine peptidases (Supplemental Figure S7). In the leupeptin experiment, we obtained the turnover for 386 proteins and the overlap with the proteins found in common in the DMOG/untreated experiment was 148 proteins (Supplemental Tables S4–S7). The inhibition of protein degradation by leupeptin most likely reflects the turnover of the majority of the cellular proteins degraded by lysosomes, including those degraded by autophagy, and the ones localized in mitochondria also degraded by calpains and other serine proteases, further suggesting a prominent role for reactive oxygen species in regulating overall protein turnover.

## DISCUSSION

Herein, we have investigated the role of protein turnover for cellular adaptation during metabolic reprogramming to an enhanced aerobic glycolysis using DMOG, an inhibitor of prolyl-hydroxylases. In agreement with previous findings in cardiomyocytes,[12] cancer cells[14] and bone marrow-derived angiogenic cells,[5] DMOG induced HIF-1$\alpha$ expression, inhibited mitochondrial respiration, promoted aerobic glycolysis and stimulated cellular proliferation of colon cancer cells.[6] These findings are in agreement with a previous study that showed that proliferation of colon cancer cells requires the selection of cells with a highly glycolytic phenotype.[26] Interestingly, DMOG inhibited CDK1 phosphorylation which is sufficient to drive cell cycle progression.[54] Moreover, CDK1 has been shown to contribute to the stability and transcriptional activity of HIF-1$\alpha$ by blocking its lysosomal degradation.[55]

As an exploratory attempt to investigate the potential implication of protein turnover in metabolic reprogramming, we first studied by a conventional approach the synthesis and



DOI: 10.1021/acs.jproteome.9b00239
J. Proteome Res. 2019, 18, 3142−3155

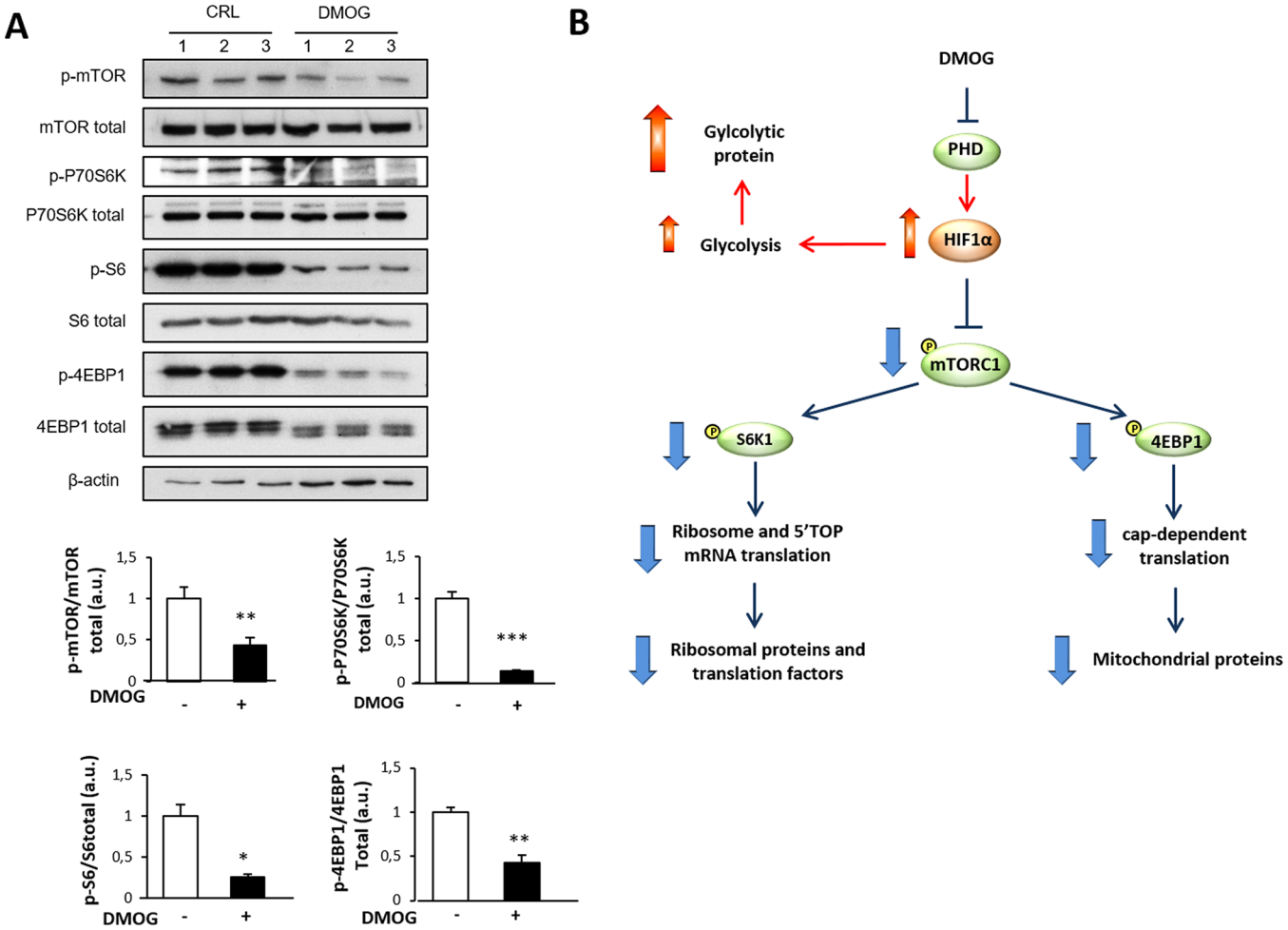


**Figure 7.** DMOG inhibits the mTORC1 signaling pathway. HCT116 cells were treated with 1 mM DMOG for 24 h or left untreated. (A) Western blot analysis of the expression of p-mTORC1, mTORC1, p-p70S6K, p70S6K, p-S6, S6, p-4EBP1, and 4EBP1 in three different preparations. $\beta$-actin is shown as loading control. The histograms show the quantification of the bands (a.u.) normalized to the mean value in untreated cells. The results shown are means ± SEM ($n$ = 3). *$p$ < 0.05, **$p$ < 0.01, and ***$p$ < 0.001, when compared to nontreated by Student's $t$ test. (B) The scheme summarizes the effects of DMOG-mediated reprogramming in the turnover of glycolytic, mitochondrial and ribosomal proteins and translation factors. PHD, prolyl-hydroxylases; HIF-1$\alpha$, Hypoxia inducible factor 1$\alpha$; mTORC1, mammalian target of rapamycin complex 1; S6K1, S6 kinase 1; 4EBP1, eIF4E binding protein 1.

turnover of the mitochondrial $\beta$-F1-ATPase protein of OXPHOS and GAPDH of glycolysis. These proteins respectively represent biomarkers that estimate the relative changes of OXPHOS and glycolysis during metabolic reprogramming as defined in the "bioenergetic signature".[56−59] Consistent with the onset of metabolic reprogramming, DMOG triggered the inhibition of the synthesis of $\beta$-F1-ATPase and the concurrent enhanced synthesis of GAPDH. Similar findings on the synthesis of both proteins have been obtained when reprogramming was induced by oligomycin treatment.[28] Moreover, these changes were paralleled by an increase in the stability of the mitochondrial $\beta$-F1-ATPase, whereas the turnover of the glycolytic GAPDH was significantly accelerated. Interestingly, and despite the rapid and opposite changes in the synthesis and turnover of the two enzymes of energy metabolism, the steady state expression of the two proteins was not affected after 48 h of DMOG treatment. These findings contrasted with the sharp reduction of the steady-state expression of mitochondrial proteins in response to oligomycin treatment,[28] suggesting that changes in the "bioenergetic signature" of the cell requires a sustained and long-term pressure on the metabolic proteome for reprogramming.

On the basis of the above exploratory results we investigated the turnover of the cellular proteome by a high-throughput dynamic SILAC approach[36,60,61] during DMOG-induced reprogramming. Of note, most of the proteins that showed significant changes in turnover were stabilized by DMOG treatment in differentiated cardiomyocytes,[62] suggesting a relevant role for prolyl-hydroxylases in proteostasis. In agreement with these authors, we observed that 51% of the proteins identified in our study become stabilized by DMOG treatment. Proteins in common between both studies are chaperones (PDIA3, PDIA4, CALR, HSPB1), nucleic acid binding proteins (SFPQ, XRCC5, PCBP1) and proteins with enzymatic activity (GANAB, LDHB). On the contrary, proteins involved in glycolysis (ALDOA and GAPDH), endolysosomal trafficking (RAB7A), assembly of ribonucleoproteins (STRAP), cell adhesion (TES) and cell cycle regulation (CLIC1) showed an increase in their turnover in colon cancer cells whereas were stabilized in differentiated cardiomyocytes.[62] These differences might stem from the different metabolic requirements that exist between a differ-


DOI: 10.1021/acs.jproteome.9b00239
J. Proteome Res. 2019, 18, 3142−3155

entiated cardiomyocyte and a proliferative cancer cell. Of note, only in ∼3% of the proteins that showed a relevant change in protein turnover as a result of DMOG treatment showed nonhydroxylated proline residues in their tryptic peptides.

Following the stringent criteria in the selection of the proteins included in the study, the major subcellular proteomes affected by stabilization were those involved in protein synthesis and mitochondrial OXPHOS and metabolism. Specifically, and regarding mitochondria, key OXPHOS proteins that showed significantly reduced turnover rates in cells treated with DMOG included components of the respiratory chain (UQCRC2, CYCS), ATP synthase (ATP5F1, ATP5B, ATP5A), phosphate and adenine nucleotide transporters (SLC25A3, SLC25A5), metabolic enzymes (GOT2, MDH2, SHMT2, AK2) and molecular chaperones (HSPA9, HSPE1, HSPD1). In contrast, relevant proteins that showed a significant increase in its turnover upon DMOG treatment were enzymes of the glycolytic pathway (GPI, ALDOA, ENO1, GAPDH), confirming and further emphasizing the opposite and rapid regulation of the turnover of mitochondrial and glycolytic proteins during metabolic reprogramming.

The regulation of the expression of OXPHOS genes is exerted at post-transcriptional levels during development, differentiation and in oncogenesis.[63−65] Consistently, the changes in protein turnover triggered by DMOG on mitochondrial proteins are not paralleled by changes in mRNA abundance. In contrast, we found that the half-life of the cluster of glycolytic enzymes studied inversely correlates with the cellular availability of their mRNAs in response to DMOG, suggesting a link between the rate of protein turnover and the transcriptional response. Overall, and in agreement with previous findings by others, there is partial correlation between mRNA levels and protein expression and turnover. Remarkably, the inhibition of mitochondrial respiration and the activation of aerobic glycolysis respectively correlated with the stabilization of the turnover of mitochondrial proteins and the activation of the turnover of glycolytic enzymes, supporting that the metabolic flux through a given pathway correlates with changes in the turnover of the proteins involved. These results suggest the idea that the renewal of proteins is enhanced when the metabolic pathway is activated. In other words, the metabolic activity determines enzymes' half-life.

Although our results indicate a rather general DMOG-mediated shutdown of protein synthesis and concurrent protein stabilization of different cellular compartments, the inhibition is selective because the translation and turnover of glycolytic proteins is enhanced. mTORC1 is a master regulator of protein synthesis whose activation positively controls cap-dependent translation, ribosome biogenesis[18,66] and the maintenance of the bioenergetic function of mitochondria.[28,67,68] Consistent with our findings, DMOG treatment significantly repressed the mTORC1 pathway as revealed by its diminished phosphorylation and that of its downstream targets p70S6K and 4EBP1, which control the biosynthesis of ribosomes and the 5′-cap dependent translation of nuclear encoded mitochondrial mRNAs (Figure 7B).[69] Overall, these results emphasize the relevance of the inhibition of mTORC1 pathway in controlling protein synthesis and turnover for metabolic adaptation to an enhanced glycolytic phenotype. Recent findings have stressed the relevance of a diminished hypusination of the translation initiation factor eIF5A in metabolic reprogramming to an enhanced glycolysis, to confer resistance to anoxic cell death by inhibiting the synthesis of nuclear encoded mitochondrial proteins.[70] In this regard, we cannot ruled out the participation of DMOG elicited HIF-1$\alpha$-independent mechanisms[71−73] that might affect eIF5A hypusination in silencing the synthesis of mitochondrial proteins during reprogramming.

On the contrary, the synthesis and turnover of glycolytic enzymes are significantly stimulated upon DMOG treatment strongly emphasizing the differential regulation of the two main pathways of energy metabolism during metabolic reprogramming. Indeed, we found that whereas the synthesis of mitochondrial proteins is largely mTORC1-dependent through cap-dependent translation the synthesis of glycolytic enzymes is not. It is tempting to suggest that the synthesis of glycolytic enzymes shares signaling pathways and mechanisms with proteins involved in cellular adaptation to stressful conditions.[74,75]

Consistent with the role of serine-proteases in controlling protein degradation[76] we observed that incubation of the cells with leupeptin triggered a ∼2 fold increase in the stability of all the subcellular proteomes investigated. Mitochondria are primary signaling hubs of the cell,[50,77] and mtROS represent a relevant signaling molecule that emanates from its activity affecting both cell fate and behavior.[48−50] Hence, we interrogated whether the mtROS produced in response to the inhibition of prolyl hydroxylases could be involved in regulating protein turnover. Remarkably, we found that in control non-DMOG treated cells, MitoQ already stabilized all the subcellular proteomes of the cells to the same level as leupeptin irrespective of DMOG treatment. Since MitoQ is unlikely to affect the activity of serine proteases, our results suggest that the basal oxidation of cellular proteins is a main determinant controlling protein turnover, being the mtROS produced in response to DMOG treatment of marginal relevance in this situation.

The contribution of the different protein degradation pathways that are activated/repressed during reprogramming deserve future investigations because of the prominent role played by proteostasis in aging and age-related diseases.[18,44,77] In this regard, and in agreement with our results of an enhanced turnover of mitochondrial proteins when OXPHOS is activated, it has been described that the stimulation of OXPHOS enhances Rheb-dependent mitophagy,[78,79] a mechanism to promote renewal of the organelles to ensure optimal mitochondrial energy production. Alternatively, the PINK1-Parkin pathway that mediates the selective turnover of proteins of the mitochondrial respiratory chain[80] could also be involved in promoting the selective degradation of these proteins upon activation of OXPHOS. Since autophagy is enhanced in colon cancer cells that rewire its metabolism to an increased glycolysis,[28] it is quite likely the implication of this pathway in facilitating the renewal of specific proteins during reprogramming.

To summarize, our findings strongly support that switching energy metabolism from mitochondrial OXPHOS to aerobic glycolysis requires a profound and opposite change in the regulation of the turnover of glycolytic and mitochondrial proteins. Inhibition of the mTORC1 signaling pathway gears the partial silencing of the synthesis and stabilization of mitochondrial and ribosomal proteins during reprogramming. Finally, the basal production of mtROS seem to play a fundamental role in defining the overall turnover of the cellular proteome.



DOI: 10.1021/acs.jproteome.9b00239
J. Proteome Res. 2019, 18, 3142−3155

## CONCLUSIONS

The turnover of different subcellular proteomes is significantly altered during metabolic reprogramming to an enhanced DMOG-mediated glycolytic phenotype. Specifically, inhibition of the mTOR pathway seems to gear the stabilization of the majority of mitochondrial and ribosomal proteins and translation initiation factors. In contrast, the synthesis and turnover of glycolytic enzymes is significantly accelerated during reprogramming by an mTOR-independent mechanism. The overall turnover of the proteome is profoundly stabilized by inhibitors of serine-proteases and by a mitochondrial targeted antioxidant.

### Information of Proteomic experiments

The mass spectrometry proteomics data have been deposited to the ProteomeXchange Consortium via the PRIDE partner repository with the data set identifier PXD013482 and 10.6019/PXD013482. Further details are described in the Supporting Information.

## ASSOCIATED CONTENT

### Supporting Information

The Supporting Information is available free of charge on the ACS Publications website at DOI: 10.1021/acs.jproteome.9b00239.

Figures S1−S7 (PDF)

Table S1: Proteins with an increase in the half-life in DMOG-treated when compared to control cells; F.C., Fold change; DMOG/CRL ≥ 1.20 (XLSX)

Table S2: Proteins with a decreased in the half-life in DMOG-treated when compared to control cells; F.C., Fold change; DMOG/CRL < 0.80 (XLSX)

Table S3: Proteins without significant changes in the half-life between DMOG-treated and control cells; F.C., Fold change; DMOG/CRL ≤ 1.20 and ≥ 0.80 (XLSX)

Table S4: Half-life (h) of mitochondrial proteins in control (CRL); CRL MitoQ-treated (MitoQ), DMOG, DMOG+MitoQ and leupeptin treated cells for the indicated condition and experiment (XLSX)

Table S5: Half-life (h) of ribosomal proteins in control (CRL); CRL MitoQ-treated (MitoQ), DMOG, DMOG +MitoQ and leupeptin treated cells for the indicated condition and experiment (XLSX)

Table S6: Half-life (h) of glycolytic proteins in control (CRL); CRL MitoQ treated (MitoQ), DMOG, DMOG +MitoQ and leupeptin treated cells for the indicated condition and experiment (XLSX)

Table S7: Half-life (h) of translation factors in control (CRL); CRL MitoQ treated (MitoQ), DMOG, DMOG +MitoQ and leupeptin treated cells for the indicated condition and experiment (XLSX)

Additional Western blots (PDF)

## AUTHOR INFORMATION


### Corresponding Author

*Phone: 34-91 196 4618. Fax: 34-91 196 4420. E-mail: jmcuezva@cbm.csic.es.

### ORCID

Ana García-Aguilar: 0000-0003-1648-7143

Inmaculada Martínez-Reyes: 0000-0003-0479-1535

José M. Cuezva: 0000-0003-1118-248X


### Author Contributions

†AGA and IMR contributed equally. AGA and IMR performed research. AGA, IMR, and JMC designed research, analyzed data, and wrote the paper. All authors read, contributed, and approved the final manuscript.

### Notes

The authors declare no competing financial interest.

## ACKNOWLEDGMENTS

The authors thank Drs. A.I. Marina and E. Morato of the Proteomic Facility of the CBMSO, which is a member of ProteoRed. ProteoRed-ISCIII is a networked proteomics initiative within the Biomolecular Resources Platform (PRB3) of the Spanish National Institutes of Health ISCIII supported by grant PT17/0019. The authors also thank CNB-CSIC lab member of Proteored. The authors also thank the excellent technical assistance of Cristina Núñez de Arenas and Brenda Sánchez-Garrido. The work was supported by grants from MINECO (SAF2013-41945-R and SAF2016-75916-R), CIBERER-ISCIII, and Fundación Ramón Areces, Spain.

## REFERENCES


(1) Vander Heiden, M. G.; Cantley, L. C.; Thompson, C. B. Understanding the Warburg effect: the metabolic requirements of cell proliferation. *Science* **2009**, *324* (5930), 1029−33.

(2) Hanahan, D.; Weinberg, R. A. Hallmarks of cancer: the next generation. *Cell* **2011**, *144* (5), 646−74.

(3) Lunt, S. Y.; Vander Heiden, M. G. Aerobic glycolysis: meeting the metabolic requirements of cell proliferation. *Annu. Rev. Cell Dev. Biol.* **2011**, *27*, 441−64.

(4) Masoud, G. N.; Li, W. HIF-1alpha pathway: role, regulation and intervention for cancer therapy. *Acta Pharm. Sin. B* **2015**, *5* (5), 378−89.

(5) Rey, S.; Luo, W.; Shimoda, L. A.; Semenza, G. L. Metabolic reprogramming by HIF-1 promotes the survival of bone marrow-derived angiogenic cells in ischemic tissue. *Blood* **2011**, *117* (18), 4988−98.

(6) Dang, D. T.; Chen, F.; Gardner, L. B.; Cummins, J. M.; Rago, C.; Bunz, F.; Kantsevoy, S. V.; Dang, L. H. Hypoxia-inducible factor-1alpha promotes nonhypoxia-mediated proliferation in colon cancer cells and xenografts. *Cancer Res.* **2006**, *66* (3), 1684−936.

(7) Semenza, G. L.; Nejfelt, M. K.; Chi, S. M.; Antonarakis, S. E. Hypoxia-inducible nuclear factors bind to an enhancer element located 3′ to the human erythropoietin gene. *Proc. Natl. Acad. Sci. U. S. A.* **1991**, *88* (13), 5680−5684.

(8) Jones, R. G.; Thompson, C. B. Tumor suppressors and cell metabolism: a recipe for cancer growth. *Genes Dev.* **2009**, *23* (5), 537−48.

(9) Bruick, R. K.; McKnight, S. L. A conserved family of prolyl-4-hydroxylases that modify HIF. *Science* **2001**, *294* (5545), 1337−40.

(10) Maxwell, P. H.; Wiesener, M. S.; Chang, G. W.; Clifford, S. C.; Vaux, E. C.; Cockman, M. E.; Wykoff, C. C.; Pugh, C. W.; Maher, E. R.; Ratcliffe, P. J. The tumour suppressor protein VHL targets hypoxia-inducible factors for oxygen-dependent proteolysis. *Nature* **1999**, *399* (6733), 271−5.

(11) Salceda, S.; Caro, J. Hypoxia-inducible factor 1alpha (HIF-1alpha) protein is rapidly degraded by the ubiquitin-proteasome system under normoxic conditions. Its stabilization by hypoxia depends on redox-induced changes. *J. Biol. Chem.* **1997**, *272* (36), 22642−7.

(12) Sridharan, V.; Guichard, J.; Li, C. Y.; Muise-Helmericks, R.; Beeson, C. C.; Wright, G. L. O(2)-sensing signal cascade: clamping of O(2) respiration, reduced ATP utilization, and inducible fumarate respiration. *Am. J. Physiol Cell Physiol* **2008**, *295* (1), C29−37.

(13) Takahashi, E.; Sato, M. Anaerobic respiration sustains mitochondrial membrane potential in a prolyl hydroxylase pathway-




DOI: 10.1021/acs.jproteome.9b00239
J. Proteome Res. 2019, 18, 3142−3155

activated cancer cell line in a hypoxic microenvironment. *Am. J. Physiol Cell Physiol* **2014**, *306* (4), C334−42.
(14) Zhdanov, A. V.; Okkelman, I. A.; Collins, F. W.; Melgar, S.; Papkovsky, D. B. A novel effect of DMOG on cell metabolism: direct inhibition of mitochondrial function precedes HIF target gene expression. *Biochim. Biophys. Acta, Bioenerg.* **2015**, *1847* (10), 1254−66.
(15) Goldberg, A. L.; St. John, A. C. Intracellular protein degradation in mammalian and bacterial cells: Part 2. *Annu. Rev. Biochem.* **1976**, *45*, 747−803.
(16) Brehme, M.; Voisine, C.; Rolland, T.; Wachi, S.; Soper, J. H.; Zhu, Y.; Orton, K.; Villella, A.; Garza, D.; Vidal, M.; Ge, H.; Morimoto, R. I. A chaperome subnetwork safeguards proteostasis in aging and neurodegenerative disease. *Cell Rep.* **2014**, *9* (3), 1135−50.
(17) Yi, T.; Papadopoulos, E.; Hagner, P. R.; Wagner, G. Hypoxia-inducible factor-1alpha (HIF-1alpha) promotes cap-dependent translation of selective mRNAs through up-regulating initiation factor eIF4E1 in breast cancer cells under hypoxia conditions. *J. Biol. Chem.* **2013**, *288* (26), 18732−42.
(18) Zhang, Y.; Nicholatos, J.; Dreier, J. R.; Ricoult, S. J.; Widenmaier, S. B.; Hotamisligil, G. S.; Kwiatkowski, D. J.; Manning, B. D. Coordinated regulation of protein synthesis and degradation by mTORC1. *Nature* **2014**, *513* (7518), 440−3.
(19) Zhao, J.; Zhai, B.; Gygi, S. P.; Goldberg, A. L. mTOR inhibition activates overall protein degradation by the ubiquitin proteasome system as well as by autophagy. *Proc. Natl. Acad. Sci. U. S. A.* **2015**, *112* (52), 15790−7.
(20) Pratt, J. M.; Petty, J.; Riba-Garcia, I.; Robertson, D. H.; Gaskell, S. J.; Oliver, S. G.; Beynon, R. J. Dynamics of protein turnover, a missing dimension in proteomics. *Mol. Cell. Proteomics* **2002**, *1* (8), 579−91.
(21) Goldberg, A. L. Protein degradation and protection against misfolded or damaged proteins. *Nature* **2003**, *426* (6968), 895−9.
(22) Bachmair, A.; Finley, D.; Varshavsky, A. In vivo half-life of a protein is a function of its amino-terminal residue. *Science* **1986**, *234* (4773), 179−86.
(23) Dobson, C. M. Protein folding and misfolding. *Nature* **2003**, *426* (6968), 884−90.
(24) Rugarli, E. I.; Langer, T. Mitochondrial quality control: a matter of life and death for neurons. *EMBO J.* **2012**, *31* (6), 1336−49.
(25) Claydon, A. J.; Beynon, R. J. Protein turnover methods in single-celled organisms: dynamic SILAC. *Methods Mol. Biol.* **2011**, *759*, 179−95.
(26) Sanchez-Arago, M.; Chamorro, M.; Cuezva, J. M. Selection of cancer cells with repressed mitochondria triggers colon cancer progression. *Carcinogenesis* **2010**, *31* (4), 567−76.
(27) Formentini, L.; Sánchez-Aragó, M.; Sánchez-Cenizo, L.; Cuezva, J. M. The mitochondrial ATPase Inhibitory Factor 1 (IF1) triggers a ROS-mediated retrograde pro-survival and proliferative response. *Mol. Cell* **2012**, *45*, 731−742.
(28) Martinez-Reyes, I.; Sanchez-Arago, M.; Cuezva, J. M. AMPK and GCN2-ATF4 signal the repression of mitochondria in colon cancer cells. *Biochem. J.* **2012**, *444* (2), 249−59.
(29) Moreno, M. L.; Escobar, J.; Izquierdo-Alvarez, A.; Gil, A.; Perez, S.; Pereda, J.; Zapico, I.; Vento, M.; Sabater, L.; Marina, A.; Martinez-Ruiz, A.; Sastre, J. Disulfide stress: a novel type of oxidative stress in acute pancreatitis. *Free Radical Biol. Med.* **2014**, *70*, 265−77.
(30) Shevchenko, A.; Wilm, M.; Vorm, O.; Mann, M. Mass spectrometric sequencing of proteins silver-stained polyacrylamide gels. *Anal. Chem.* **1996**, *68* (5), 850−8.
(31) Alonso, R.; Pisa, D.; Marina, A. I.; Morato, E.; Rabano, A.; Rodal, I.; Carrasco, L. Evidence for fungal infection in cerebrospinal fluid and brain tissue from patients with amyotrophic lateral sclerosis. *Int. J. Biol. Sci.* **2015**, *11* (5), 546−58.
(32) Zhang, J.; Xin, L.; Shan, B.; Chen, W.; Xie, M.; Yuen, D.; Zhang, W.; Zhang, Z.; Lajoie, G. A.; Ma, B. PEAKS DB: de novo sequencing assisted database search for sensitive and accurate peptide identification. *Mol. Cell. Proteomics* **2012**, *11* (4), M111.010587.
(33) Han, X.; He, L.; Xin, L.; Shan, B.; Ma, B. PeaksPTM: Mass spectrometry-based identification of peptides with unspecified modifications. *J. Proteome Res.* **2011**, *10* (7), 2930−6.
(34) Han, Y.; Ma, B.; Zhang, K. SPIDER: software for protein identification from sequence tags with de novo sequencing error. *J. Bioinf. Comput. Biol.* **2005**, *03*, 697.
(35) de Godoy, L. M.; Olsen, J. V.; Cox, J.; Nielsen, M. L.; Hubner, N. C.; Frohlich, F.; Walther, T. C.; Mann, M. Comprehensive mass-spectrometry-based proteome quantification of haploid versus diploid yeast. *Nature* **2008**, *455* (7217), 1251−4.
(36) Doherty, M. K.; Hammond, D. E.; Clague, M. J.; Gaskell, S. J.; Beynon, R. J. Turnover of the human proteome: determination of protein intracellular stability by dynamic SILAC. *J. Proteome Res.* **2009**, *8* (1), 104−12.
(37) Sandoval, P. C.; Slentz, D. H.; Pisitkun, T.; Saeed, F.; Hoffert, J. D.; Knepper, M. A. Proteome-wide measurement of protein half-lives and translation rates in vasopressin-sensitive collecting duct cells. *J. Am. Soc. Nephrol.* **2013**, *24* (11), 1793−805.
(38) Tabas-Madrid, D.; Nogales-Cadenas, R.; Pascual-Montano, A. GeneCodis3: a non-redundant and modular enrichment analysis tool for functional genomics. *Nucleic Acids Res.* **2012**, *40*, W478−W483.
(39) Nogales-Cadenas, R.; Carmona-Saez, P.; Vazquez, M.; Vicente, C.; Yang, X.; Tirado, F.; Carazo, J. M.; Pascual-Montano, A. GeneCodis: interpreting gene lists through enrichment analysis and integration of diverse biological information. *Nucleic Acids Res.* **2009**, *37*, W317−W322.
(40) Carmona-Saez, P.; Chagoyen, M.; Tirado, F.; Carazo, J. M.; Pascual-Montano, A. GENECODIS: a web-based tool for finding significant concurrent annotations in gene lists. *Genome Biol.* **2007**, *8* (1), R3.
(41) Lopez-Ferrer, D.; Martinez-Bartolome, S.; Villar, M.; Campillos, M.; Martin-Maroto, F.; Vazquez, J. Statistical model for large-scale peptide identification in databases from tandem mass spectra using SEQUEST. *Anal. Chem.* **2004**, *76* (23), 6853−60.
(42) Semenza, G. L. Hypoxia-inducible factors: mediators of cancer progression and targets for cancer therapy. *Trends Pharmacol. Sci.* **2012**, *33* (4), 207−14.
(43) Aragones, J.; Schneider, M.; Van Geyte, K.; Fraisl, P.; Dresselaers, T.; Mazzone, M.; Dirkx, R.; Zacchigna, S.; Lemieux, H.; Jeoung, N. H.; Lambrechts, D.; Bishop, T.; Lafuste, P.; Diez-Juan, A.; Harten, S. K.; Van Noten, P.; De Bock, K.; Willam, C.; Tjwa, M.; Grosfeld, A.; Navet, R.; Moons, L.; Vandendriessche, T.; Deroose, C.; Wijeyekoon, B.; Nuyts, J.; Jordan, B.; Silasi-Mansat, R.; Lupu, F.; Dewerchin, M.; Pugh, C.; Salmon, P.; Mortelmans, L.; Gallez, B.; Gorus, F.; Buyse, J.; Sluse, F.; Harris, R. A.; Gnaiger, E.; Hespel, P.; Van Hecke, P.; Schuit, F.; Van Veldhoven, P.; Ratcliffe, P.; Baes, M.; Maxwell, P.; Carmeliet, P. Deficiency or inhibition of oxygen sensor Phd1 induces hypoxia tolerance by reprogramming basal metabolism. *Nat. Genet.* **2008**, *40* (2), 170−80.
(44) Sonenberg, N.; Hinnebusch, A. G. Regulation of translation initiation in eukaryotes: mechanisms and biological targets. *Cell* **2009**, *136* (4), 731−45.
(45) Laplante, M.; Sabatini, D. M. mTOR signaling at a glance. *J. Cell Sci.* **2009**, *122* (20), 3589−3594.
(46) Showkat, M.; Beigh, M. A.; Andrabi, K. I. mTOR Signaling in Protein Translation Regulation: Implications in Cancer Genesis and Therapeutic Interventions. *Mol. Biol. Int.* **2014**, *2014*, 686984.
(47) Formentini, L.; Santacatterina, F.; Nunez de Arenas, C.; Stamatakis, K.; Lopez-Martinez, D.; Logan, A.; Fresno, M.; Smits, R.; Murphy, M. P.; Cuezva, J. M. Mitochondrial ROS Production Protects the Intestine from Inflammation through Functional M2Macrophage Polarization. *Cell Rep.* **2017**, *19* (6), 1202−1213.
(48) Garcia-Aguilar, A.; Cuezva, J. M. A Review of the Inhibition of the Mitochondrial ATP Synthase by IF1 in vivo: Reprogramming Energy Metabolism and Inducing Mitohormesis. *Front. Physiol.* **2018**, *9*, 1322.
(49) Shadel, G. S.; Horvath, T. L. Mitochondrial ROS Signaling in Organismal Homeostasis. *Cell* **2015**, *163* (3), 560−9.


DOI: 10.1021/acs.jproteome.9b00239
*J. Proteome Res.* 2019, 18, 3142−3155

(50) Chandel, N. S. Evolution of Mitochondria as Signaling Organelles. *Cell Metab.* **2015**, *22* (2), 204−6.
(51) Brunelle, J. K.; Bell, E. L.; Quesada, N. M.; Vercauteren, K.; Tiranti, V.; Zeviani, M.; Scarpulla, R. C.; Chandel, N. S. Oxygen sensing requires mitochondrial ROS but not oxidative phosphorylation. *Cell Metab.* **2005**, *1* (6), 409−14.
(52) Mansfield, K. D.; Guzy, R. D.; Pan, Y.; Young, R. M.; Cash, T. P.; Schumacker, P. T.; Simon, M. C. Mitochondrial dysfunction resulting from loss of cytochrome c impairs cellular oxygen sensing and hypoxic HIF-alpha activation. *Cell Metab.* **2005**, *1* (6), 393−9.
(53) Guzy, R. D.; Hoyos, B.; Robin, E.; Chen, H.; Liu, L.; Mansfield, K. D.; Simon, M. C.; Hammerling, U.; Schumacker, P. T. Mitochondrial complex III is required for hypoxia-induced ROS production and cellular oxygen sensing. *Cell Metab.* **2005**, *1* (6), 401−8.
(54) Santamaria, D.; Barriere, C.; Cerqueira, A.; Hunt, S.; Tardy, C.; Newton, K.; Caceres, J. F.; Dubus, P.; Malumbres, M.; Barbacid, M. Cdk1 is sufficient to drive the mammalian cell cycle. *Nature* **2007**, *448* (7155), 811−5.
(55) Hubbi, M. E.; Gilkes, D. M.; Hu, H.; Kshitiz Ahmed, I.; Semenza, G. L. Cyclin-dependent kinases regulate lysosomal degradation of hypoxia-inducible factor 1alpha to promote cell-cycle progression. *Proc. Natl. Acad. Sci. U. S. A.* **2014**, *111* (32), E3325−E3334.
(56) Cuezva, J. M.; Chen, G.; Alonso, A. M.; Isidoro, A.; Misek, D. E.; Hanash, S. M.; Beer, D. G. The bioenergetic signature of lung adenocarcinomas is a molecular marker of cancer diagnosis and prognosis. *Carcinogenesis* **2004**, *25* (7), 1157−63.
(57) Cuezva, J. M.; Krajewska, M.; de Heredia, M. L.; Krajewski, S.; Santamaria, G.; Kim, H.; Zapata, J. M.; Marusawa, H.; Chamorro, M.; Reed, J. C. The bioenergetic signature of cancer: a marker of tumor progression. *Cancer Res.* **2002**, *62* (22), 6674−6681.
(58) Lopez-Rios, F.; Sanchez-Arago, M.; Garcia-Garcia, E.; Ortega, A. D.; Berrendero, J. R.; Pozo-Rodriguez, F.; Lopez-Encuentra, A.; Ballestin, C.; Cuezva, J. M. Loss of the mitochondrial bioenergetic capacity underlies the glucose avidity of carcinomas. *Cancer Res.* **2007**, *67* (19), 9013−7.
(59) Yizhak, K.; Le Devedec, S. E.; Rogkoti, V. M.; Baenke, F.; de Boer, V. C.; Frezza, C.; Schulze, A.; van de Water, B.; Ruppin, E. A computational study of the Warburg effect identifies metabolic targets inhibiting cancer migration. *Mol. Syst. Biol.* **2014**, *10*, 744.
(60) Mathieson, T.; Franken, H.; Kosinski, J.; Kurzawa, N.; Zinn, N.; Sweetman, G.; Poeckel, D.; Ratnu, V. S.; Schramm, M.; Becher, I.; Steidel, M.; Noh, K. M.; Bergamini, G.; Beck, M.; Bantscheff, M.; Savitski, M. M. Systematic analysis of protein turnover in primary cells. *Nat. Commun.* **2018**, *9* (1), 689.
(61) Boisvert, F. M.; Ahmad, Y.; Gierlinski, M.; Charriere, F.; Lamont, D.; Scott, M.; Barton, G.; Lamond, A. I. A quantitative spatial proteomics analysis of proteome turnover in human cells. *Mol. Cell. Proteomics* **2012**, *11* (3), M111.011429.
(62) Stoehr, A.; Yang, Y.; Patel, S.; Evangelista, A. M.; Aponte, A.; Wang, G.; Liu, P.; Boylston, J.; Kloner, P. H.; Lin, Y.; Gucek, M.; Zhu, J.; Murphy, E. Prolyl hydroxylation regulates protein degradation, synthesis, and splicing in human induced pluripotent stem cell-derived cardiomyocytes. *Cardiovasc. Res.* **2016**, *110* (3), 346−58.
(63) Luis, A. M.; Izquierdo, J. M.; Ostronoff, L. K.; Salinas, M.; Santaren, J. F.; Cuezva, J. M. Translational regulation of mitochondrial differentiation in neonatal rat liver. Specific increase in the translational efficiency of the nuclear-encoded mitochondrial beta-F1-ATPase mRNA. *J. Biol. Chem.* **1993**, *268* (3), 1868−1875.
(64) Willers, I. M.; Cuezva, J. M. Post-transcriptional regulation of the mitochondrial H(+)-ATP synthase: A key regulator of the metabolic phenotype in cancer. *Biochim. Biophys. Acta, Bioenerg.* **2011**, *1807* (6), 543−51.
(65) Sanchez-Arago, M.; Garcia-Bermudez, J.; Martinez-Reyes, I.; Santacatterina, F.; Cuezva, J. M. Degradation of IF1 controls energy metabolism during osteogenic differentiation of stem cells. *EMBO Rep.* **2013**, *14* (7), 638−44.
(66) Thoreen, C. C.; Chantranupong, L.; Keys, H. R.; Wang, T.; Gray, N. S.; Sabatini, D. M. A unifying model for mTORC1-mediated regulation of mRNA translation. *Nature* **2012**, *485* (7396), 109−13.
(67) Schieke, S. M.; Phillips, D.; McCoy, J. P., Jr.; Aponte, A. M.; Shen, R. F.; Balaban, R. S.; Finkel, T. The mammalian target of rapamycin (mTOR) pathway regulates mitochondrial oxygen consumption and oxidative capacity. *J. Biol. Chem.* **2006**, *281* (37), 27643−52.
(68) Morita, M.; Gravel, S. P.; Chenard, V.; Sikstrom, K.; Zheng, L.; Alain, T.; Gandin, V.; Avizonis, D.; Arguello, M.; Zakaria, C.; McLaughlan, S.; Nouet, Y.; Pause, A.; Pollak, M.; Gottlieb, E.; Larsson, O.; St-Pierre, J.; Topisirovic, I.; Sonenberg, N. mTORC1 controls mitochondrial activity and biogenesis through 4E-BP-dependent translational regulation. *Cell Metab.* **2013**, *18* (5), 698−711.
(69) Gentilella, A.; Kozma, S. C.; Thomas, G. A liaison between mTOR signaling, ribosome biogenesis and cancer. *Biochim. Biophys. Acta, Gene Regul. Mech.* **2015**, *1849* (7), 812−20.
(70) Melis, N.; Rubera, I.; Cougnon, M.; Giraud, S.; Mograbi, B.; Belaid, A.; Pisani, D. F.; Huber, S. M.; Lacas-Gervais, S.; Fragaki, K.; Blondeau, N.; Vigne, P.; Frelin, C.; Hauet, T.; Duranton, C.; Tauc, M. Targeting eIF5A Hypusination Prevents Anoxic Cell Death through Mitochondrial Silencing and Improves Kidney Transplant Outcome. *J. Am. Soc. Nephrol.* **2017**, *28* (3), 811−822.
(71) Elvidge, G. P.; Glenny, L.; Appelhoff, R. J.; Ratcliffe, P. J.; Ragoussis, J.; Gleadle, J. M. Concordant regulation of gene expression by hypoxia and 2-oxoglutarate-dependent dioxygenase inhibition: the role of HIF-1alpha, HIF-2alpha, and other pathways. *J. Biol. Chem.* **2006**, *281* (22), 15215−26.
(72) Fets, L.; Driscoll, P. C.; Grimm, F.; Jain, A.; Nunes, P. M.; Gounis, M.; Doglioni, G.; Papageorgiou, G.; Ragan, T. J.; Campos, S.; Silva Dos Santos, M.; MacRae, J. I.; O'Reilly, N.; Wright, A. J.; Benes, C. H.; Courtney, K. D.; House, D.; Anastasiou, D. MCT2 mediates concentration-dependent inhibition of glutamine metabolism by MOG. *Nat. Chem. Biol.* **2018**, *14* (11), 1032−1042.
(73) Duran, R. V.; MacKenzie, E. D.; Boulahbel, H.; Frezza, C.; Heiserich, L.; Tardito, S.; Bussolati, O.; Rocha, S.; Hall, M. N.; Gottlieb, E. HIF-independent role of prolyl hydroxylases in the cellular response to amino acids. *Oncogene* **2013**, *32* (38), 4549−56.
(74) Harding, H. P.; Novoa, I.; Zhang, Y.; Zeng, H.; Wek, R.; Schapira, M.; Ron, D. Regulated translation initiation controls stress-induced gene expression in mammalian cells. *Mol. Cell* **2000**, *6* (5), 1099−108.
(75) Walters, B.; Thompson, S. R. Cap-Independent Translational Control of Carcinogenesis. *Front. Oncol.* **2016**, *6*, 128.
(76) Libby, P.; Goldberg, A. L. Leupeptin, a protease inhibitor, decreases protein degradation in normal and diseased muscles. *Science* **1978**, *199* (4328), 534−6.
(77) Quiros, P. M.; Mottis, A.; Auwerx, J. Mitonuclear communication in homeostasis and stress. *Nat. Rev. Mol. Cell Biol.* **2016**, *17* (4), 213−26.
(78) Melser, S.; Chatelain, E. H.; Lavie, J.; Mahfouf, W.; Jose, C.; Obre, E.; Goorden, S.; Priault, M.; Elgersma, Y.; Rezvani, H. R.; Rossignol, R.; Benard, G. Rheb regulates mitophagy induced by mitochondrial energetic status. *Cell Metab.* **2013**, *17* (5), 719−30.
(79) Mishra, P.; Chan, D. C. Metabolic regulation of mitochondrial dynamics. *J. Cell Biol.* **2016**, *212* (4), 379−87.
(80) Vincow, E. S.; Merrihew, G.; Thomas, R. E.; Shulman, N. J.; Beyer, R. P.; Maccoss, M. J.; Pallanck, L. J. The PINK1-Parkin pathway promotes both mitophagy and selective respiratory chain turnover in vivo. *Proc. Natl. Acad. Sci. U. S. A.* **2013**, *110* (16), 6400−5.


DOI: 10.1021/acs.jproteome.9b00239
*J. Proteome Res.* 2019, 18, 3142−3155